TABLE 3
Biodistribution of HbV and EV as a percentage of the infused dose per organ (%ID/organ) and percentage of the infused dose per gram of organ (%ID/g organ) at 48 h after 25% top-loading in rats or rabbits

Organ	Rat		Rabbit	
	HbV	EV	HbV	EV
%ID/organ ± S.E.M.				
Blood	33.27 ± 1.11*	24.13 ± 0.65	50.95 ± 2.02†	52.76 ± 4.80‡
Liver	10.04 ± 0.86*	14.13 ± 0.40	7.55 ± 0.46†	8.64 ± 0.34‡
Bone	10.06 ± 0.21*	13.05 ± 0.38	5.37 ± 0.33*†	7.36 ± 0.28‡
Spleen	6.50 ± 0.30*	9.18 ± 0.37	0.72 ± 0.10*†	1.84 ± 0.28‡
Bowels	7.30 ± 1.59	4.16 ± 0.35	9.61 ± 2.31	8.62 ± 4.42
Skin	2.37 ± 0.33	2.29 ± 0.12	0.88 ± 0.05†	1.09 ± 0.21‡
Kidney	2.40 ± 0.10*	3.35 ± 0.08	1.47 ± 0.13†	1.69 ± 0.21‡
Muscle	1.94 ± 0.28	1.98 ± 0.27	2.51 ± 0.31	2.62 ± 0.76
Lung	0.62 ± 0.03	0.54 ± 0.03	0.55 ± 0.02	0.43 ± 0.06
Heart	0.17 ± 0.01	0.16 ± 0.01	0.12 ± 0.01†	0.13 ± 0.02
Brain	0.16 ± 0.01*	0.09 ± 0.01	0.08 ± 0.01*†	0.05 ± 0.00‡
Testis	0.12 ± 0.01*	0.09 ± 0.01	0.06 ± 0.02†	0.07 ± 0.01
Feces	9.50 ± 1.17	6.95 ± 0.29	5.06 ± 2.56	2.02 ± 0.55‡
Urine	13.61 ± 0.31	12.87 ± 0.41	11.30 ± 1.22	7.81 ± 1.44‡
%ID/g organ ± S.E.M.				
Blood	2.919 ± 0.032	1.706 ± 0.044	0.356 ± 0.017	0.354 ± 0.030
Liver	1.244 ± 0.096	1.378 ± 0.045	0.093 ± 0.004	0.131 ± 0.019
Bone	0.497 ± 0.021	0.518 ± 0.020	0.043 ± 0.003	0.062 ± 0.002
Spleen	10.059 ± 0.072	10.790 ± 0.402	0.823 ± 0.072	1.483 ± 0.072
Bowels	0.390 ± 0.073	0.202 ± 0.008	0.031 ± 0.006	0.029 ± 0.014
Skin	0.091 ± 0.014	0.070 ± 0.004	0.004 ± 0.000	0.004 ± 0.001
Kidney	1.604 ± 0.057	1.839 ± 0.055	0.089 ± 0.005	0.110 ± 0.017
Muscle	0.024 ± 0.003	0.020 ± 0.003	0.002 ± 0.000	0.002 ± 0.001
Lung	0.619 ± 0.022	0.458 ± 0.014	0.068 ± 0.004	0.057 ± 0.012
Heart	0.264 ± 0.009	0.187 ± 0.012	0.026 ± 0.002	0.027 ± 0.006
Brain	0.111 ± 0.010	0.062 ± 0.003	0.011 ± 0.001	0.006 ± 0.001
Testis	0.042 ± 0.002	0.027 ± 0.001	0.013 ± 0.002	0.016 ± 0.003

* Difference is statistically significant from EV in same species at $P < 0.01$.
† Difference is statistically significant from HbV in rat at $P < 0.05$.
‡ Difference is statistically significant from EV in rat at $P < 0.05$.

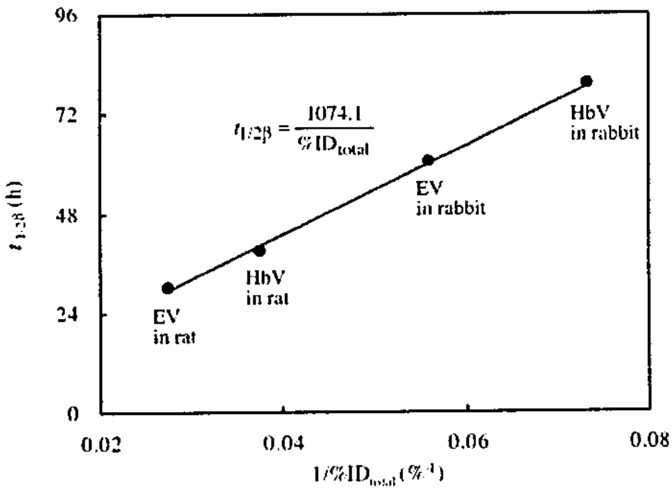

Fig. 5. Proportional relationship between the circulation half-life time ($t_{1/2\beta}$) and the reciprocal of $\%ID_{total}$ in the elimination phase. The $\%ID_{total}$ was calculated as a sum value of %ID in liver, bone, and spleen at 48 h. The fitting line was determined by the regression analysis (coefficient of determination; $R^2 = 0.9985$).

([Hb], 9.5 g/dl; [lipid], 4.75 g/dl). The normal range of human organ weight is relatively wide such as 1.4 to 1.8 kg (liver) and 0.08 to 0.3 kg (spleen), so the $t_{1/2\beta}$ would be varied around 3 days. This $t_{1/2\beta}$ is approximately two times larger than that of rat, and this ratio almost follows that derived from empirical speculation (Gabizon et al., 2003). This method of estimating vesicle circulation kinetics and organ uptake in different animal species may be useful for all types of vesicle (liposome) formulations that are currently under development as drug delivery vehicles. More studies will be required to further validate this method of estimating circulation kinetics and organ uptake in different animal species.

The development of RBC substitutes is progressing, and some modified Hbs have been studied in clinical trials. The reported $t_{1/2}$ value was 23 h for polymerized bovine Hb (Hughes et al., 1995), 16 to 20 h for *o*-raffinose-cross-linked and polymerized human Hb (Carmichael et al., 2000), and 24 h for glutaraldehyde-cross-linked and polymerized human Hb (Gould et al., 1998). Even though HbV have not yet been tested clinically, we have demonstrated in the present report that HbV have significantly improved properties, based on their circulation kinetics and biodistribution, suggesting their improved safety and efficacy as a RBC substitute. In addition, the successful application of vesicles as RBC substitutes at this large infusion dose suggests a promising future for vesicles (liposomes), and the present formulation would potentially be available not only as a RBC substitute but also for various applications such as drug delivery systems.

Acknowledgments

We gratefully acknowledge Drs. S. Takeoka and H. Sakai (Waseda University) for discussion of the experimental points and cooperation to promote this collaborative research between Waseda University and University of Texas Health Science Center at San Antonio, Y. Naito and M. Masada (Waseda University) for supporting the HbV preparation, and Dr. V. D. Awasthi (University of Texas Health Science Center at San Antonio) for advice on the experimental techniques.

TABLE 4
Comparison of HbV and EV as milligrams of lipids per gram of organ and milligrams of Hb per gram of organ at 48 h after 25% top-loading in rats or rabbits

Organ	HbV in Rat		HbV in Rabbit		EV in Rat	EV in Rabbit
	mg lipids/g organ[a]	*mg Hb/g organ*[b]	*mg lipids/g organ*[a]	*mg Hb/g organ*[b]	*mg lipids/g organ*[a]	
Blood	4.23 ± 0.20	8.40 ± 0.40	6.47 ± 0.24[†]	12.93 ± 0.48[†]	2.94 ± 0.06	6.55 ± 0.64[†]
Liver	1.79 ± 0.12	3.56 ± 0.23	1.68 ± 0.06	3.36 ± 0.12	2.38 ± 0.06	2.24 ± 0.18
Bone	0.72 ± 0.01	1.42 ± 0.02	0.78 ± 0.05	1.57 ± 0.09	0.89 ± 0.04	1.09 ± 0.08
Spleen	14.43 ± 0.54	28.63 ± 1.06	14.92 ± 1.25	29.85 ± 2.50	18.58 ± 0.51	25.83 ± 1.43[†]

[†] Difference is statistically significant from HbV in rat at $P < 0.05$.
[a] Calculated values from ID of lipids and %ID/g organ.
[b] Calculated values from ID of Hb and %ID/g organ.

References

Allen TM, Hansen C, and Rutledge J (1989) Liposomes with prolonged circulation times: factors affecting uptake by reticuloendothelial and other tissues. *Biochim Biophys Acta* **981**:27–35.

Awasthi VD, Garcia D, Goins BA, and Phillips WT (2003) Circulation and biodistribution profiles of long-circulating PEG-liposomes of various sizes in rabbits. *Int J Pharm* **253**:121–132.

Carmichael FJ, Ali AC, Campbell JA, Langlois SF, Biro GP, Willan AR, Pierce CH, and Greenburg AG (2000) A phase I study of oxidized raffinose cross-linked human hemoglobin. *Crit Care Med* **28**:2283–2292.

Dams ET, Oyen WJ, Boerman OC, Storm G, Laverman P, Kok PJ, Buijs WC, Bakker H, van der Meer JW, and Corstens FH (2000) 99mTc-PEG liposomes for the scintigraphic detection of infection and inflammation: clinical evaluation. *J Nucl Med* **41**:622–630.

Dietz AA (1944) Distribution of bone marrow, bone and bone ash in rabbits. *Proc Soc Exp Biol Med* **57**:60–62.

Djordjevich L and Miller IF (1980) Synthetic erythrocytes from lipid encapsulated hemoglobin. *Exp Hematol* **8**:584–592.

Frank DW (1976) Physiological data of laboratory animals, in *Handbook of Laboratory Animals Science* (Melby ECJ ed) pp 23–64, CRC Press, Boca Raton, FL.

Gaber BP and Farmer MC (1984) Encapsulation of hemoglobin in phospholipid vesicles: preparation and properties of a red cell surrogate. *Prog Clin Biol Res* **165**:179–190.

Gabizon A, Shmeeda H, and Barenholz Y (2003) Pharmacokinetics of pegylated liposomal doxorubicin: review of animal and human studies. *Clin Pharmacokinet* **42**:419–436.

Goda N, Suzuki K, Naito M, Takeoka S, Tsuchida E, Ishimura Y, Tamatani T, and Suematsu M (1998) Distribution of heme oxygenase isoforms in rat liver. Topographic basis for carbon monoxide-mediated microvascular relaxation. *J Clin Investig* **101**:604–612.

Goins BA and Phillips WT (2001) The use of scintigraphic imaging as a tool in the development of liposome formulations. *Prog Lipid Res* **40**:95–123.

Gould SA, Moore EE, Hoyt DB, Burch JM, Haenel JB, Garcia J, DeWoskin R, and Moss GS (1998) The first randomized trial of human polymerized hemoglobin as a blood substitute in acute trauma and emergent surgery. *J Am Coll Surg* **187**:113–122.

Gregoriadis G and Neerunjun D (1974) Control of the rate of hepatic uptake and catabolism of liposome-entrapped proteins injected into rats. Possible therapeutic applications. *Eur J Biochem* **47**:179–185.

Hughes GS Jr, Yancey EP, Albrecht R, Locker PK, Francom SF, Orringer EP, Antal EJ, and Jacobs EE Jr (1995) Hemoglobin-based oxygen carrier preserves submaximal exercise capacity in humans. *Clin Pharmacol Ther* **58**:434–443.

International Commission on Radiological Protection (1984) Report on the task group on reference man. ICRP No. 23. Pergamon Press, New York.

Kaplan HM and Timmons EH (1979) *The Rabbit: A Model for the Principles of Mammalian Physiology and Surgery*, Academic Press, New York.

Klibanov AL, Maruyama K, Torchilin VP, and Huang L (1990) Amphipathic polyethyleneglycols effectively prolong the circulation time of liposomes. *FEBS Lett* **268**:235–237.

Kozma C, Macklin W, Cummins LM, and Mauer R (1974) Anatomy, physiology, and biochemistry of the rabbit, in *The Biology of the Laboratory Rabbit* (Weisbroth SH, Flatt RE, and Kraus AL eds) pp 50–69, Academic Press, New York.

Laverman P, Brouwers AH, Dams ET, Oyen WJ, Storm G, van Rooijen N, Corstens FH, and Boerman OC (2000) Preclinical and clinical evidence for disappearance of long-circulating characteristics of polyethylene glycol liposomes at low lipid dose. *J Pharmacol Exp Ther* **293**:996–1001.

Nicholas AR, Scott MJ, Kennedy NI, and Jones MN (2000) Effect of grafted polyethylene glycol (PEG) on the size, encapsulation efficiency and permeability of vesicles. *Biochim Biophys Acta* **1463**:167–178.

Papahadjopoulos D, Allen TM, Gabizon A, Mayhew E, Matthay K, Huang SK, Lee KD, Woodle MC, Lasic DD, Redemann C, et al. (1991) Sterically stabilized liposomes: improvements in pharmacokinetics and antitumor therapeutic efficacy. *Proc Natl Acad Sci USA* **88**:11460–11464.

Perkins WR, Minchey SR, Ahl PL, and Janoff AS (1993) The determination of liposome captured volume. *Chem Phys Lipids* **64**:197–217.

Petty C (1982) *Research Techniques in the Rat*, pp 66–70, Charles C. Thomas, Springfield, IL.

Phillips WT, Klipper RW, Awasthi VD, Rudolph AS, Cliff R, Kwasiborski V, and Goins BA (1999) Polyethylene glycol-modified liposome-encapsulated hemoglobin: a long circulating red cell substitute. *J Pharmacol Exp Ther* **288**:665–670.

Phillips WT, Rudolph AS, Goins B, Timmous JH, Klipper R, and Blumhardt R (1992) A simple method for producing a technetium-99m-labeled liposome which is stable in vivo. *Nucl Med Biol* **19**:539–547.

Reinish LW, Bally MB, Loughrey HC, and Cullis PR (1988) Interactions of liposomes and platelets. *Thromb Haemost* **60**:518–523.

Rudolph AS, Klipper RW, Goins B, and Phillips WT (1991) In vivo biodistribution of a radiolabeled blood substitute: 99mTc-labeled liposome-encapsulated hemoglobin in an anesthetized rabbit. *Proc Natl Acad Sci USA* **88**:10976–10980.

Sakai H, Hisamoto S, Fukutomi I, Sou K, Takeoka S, and Tsuchida E (2004a) Detection of lipopolysaccharide in hemoglobin-vesicles by *Limulus* amebocyte lysate test with kinetic-turbidimetric gel clotting analysis and pretreatment of surfactant. *J Pharm Sci* **93**:310–321.

Sakai H, Horinouchi H, Tomiyama K, Ikeda E, Takeoka S, Kobayashi K, and Tsuchida E (2001) Hemoglobin-vesicles as oxygen carriers: influence on phagocytic activity and histopathological changes in reticuloendothelial system. *Am J Pathol* **159**:1079–1088.

Sakai H, Masada Y, Horinouchi H, Yamamoto M, Ikeda E, Takeoka S, Kobayashi K, and Tsuchida E (2004b) Hemoglobin-vesicles suspended in recombinant human serum albumin for resuscitation from hemorrhagic shock in anesthetized rats. *Crit Care Med* **32**:539–545.

Sakai H, Masada Y, Takeoka S, and Tsuchida E (2002) Characteristics opf bovine hemoglobin as a potential source of hemoglobin-vesicles for an artificial oxygen carrier. *J Biochem* **131**:611–617.

Sakai H, Tomiyama KI, Sou K, Takeoka S, and Tsuchida E (2000a) Poly(ethylene glycol)-conjugation and deoxygenation enable long-term preservation of hemoglobin-vesicles as oxygen carriers in a liquid state. *Bioconjug Chem* **11**:425–432.

Sakai H, Yuasa M, Onuma H, Takeoka S, and Tsuchida E (2000b) Synthesis and physicochemical characterization of a series of hemoglobin-based oxygen carriers: objective comparison between cellular and acellular types. *Bioconjug Chem* **11**:56–64.

Savitsky JP, Doczi J, Black J, and Arnold JD (1978) A clinical safety trial of stroma-free hemoglobin. *Clin Pharm Ther* **23**:73–80.

Sou K, Endo T, Takeoka S, and Tsuchida E (2000) Poly(ethylene glycol)-modification of the phospholipid vesicles by using the spontaneous incorporation of poly(ethylene glycol)-lipid into the vesicles. *Bioconjug Chem* **11**:372–379.

Sou K, Naito Y, Endo T, Takeoka S, and Tsuchida E (2003) Effective encapsulation of proteins into size-controlled phospholipid vesicles using the freeze-thawing and extrusion. *Biotechnol Prog* **19**:1547–1552.

Takeoka S, Ohgushi T, Terase K, Ohmori T, and Tsuchida E (1996) Layer-controlled hemoglobin vesicles by interaction of hemoglobin with a phospholipid assembly. *Langmuir* **12**:1755–1759.

Takeoka S, Teramura Y, Atoji T, and Tsuchida E (2002) Effect of Hb-encapsulation with vesicles on H_2O_2 reaction and lipid peroxidation. *Bioconjug Chem* **13**:1302–1308.

Tsuchida E (ed) (1998) *Blood Substitute: Present and Future Perspective*, Elsevier Science, Amsterdam.

Van Assendelft OW (1970) *Spectrophotometry of Haemoglobin Derivatives*, pp 125–129, Royal Vangorcum Ltd., Assen, The Netherlands.

Wakamoto S, Fujihara M, Abe H, Sakai H, Takeoka S, Tsuchida E, Ikeda H, and Ikebuchi K (2001) Effects of poly(ethyleneglycol)-modified hemoglobin vesicles on agonist-induced platelet aggregation and RANTES release in vitro. *Artif Cells Blood Substit Immobil Biotechnol* **29**:191–201.

Address correspondence to: Dr. Eishun Tsuchida, Advanced Research Institute for Science and Engineering, Waseda University, Tokyo 169-8555, Japan. E-mail: eishun@waseda.jp

tapraid4/zh4-ahea/zh4-ahea/zh400605/zh43937d05g | sweigarl | S=5 | 3/16/05 | 16:20 | MS: H1184-4 | Ini: 06e/kmp\bew | Input-dms

Am J Physiol Heart Circ Physiol 288: H000–H000, 2005.
First published January 28, 2005; doi:10.1152/ajpheart.01184.2004.

Oxygen release from low and normal P_{50} Hb vesicles in transiently occluded arterioles of the hamster window model

Hiromi Sakai,[1] Pedro Cabrales,[2,3] Amy G. Tsai,[2,3] Eishun Tsuchida,[1] and Marcos Intaglietta[2,3]

[1]*Advanced Research Institute for Science and Engineering, Waseda University, Tokyo, Japan; and* [2]*Department of Bioengineering, University of California-San Diego, and* [3]*La Jolla Bioengineering Institute, La Jolla, California*

Submitted 27 November 2004; accepted in final form 24 January 2005

Sakai, Hiromi, Pedro Cabrales, Amy G. Tsai, Eishun Tsuchida, and Marcos Intaglietta. Oxygen release from low and normal P_{50} Hb vesicles in transiently occluded arterioles of the hamster window model. *Am J Physiol Heart Circ Physiol* 288: H000–H000, 2005. First published January 28, 2005; doi:10.1152/ajpheart.01184.2004.—A phospholipid vesicle encapsulating Hb [Hb vesicle (HbV)] has been developed as a transfusion alternative. One characteristic of HbV is that the O_2 affinity [Po_2 at which Hb is 50% saturated (P_{50})] of Hb can be easily regulated by the amount of the coencapsulated allosteric effector pyridoxal 5′-phosphate. In this study, we prepared two HbVs with different P_{50}s (8 and 29 mmHg, termed HbV_8 and HbV_{29}, respectively) and observed their O_2-releasing behavior from an occluded arteriole in a hamster skinfold window model. Conscious hamsters received HbV_8 or HbV_{29} at a dose rate of 7 ml/kg. In the microscopic view, an arteriole (diameter: 53.0 ± 6.6 μm) was occluded transcutaneously by a glass pipette on a manipulator, and the reduction of the intra-arteriolar Po_2 100 μm down from the occlusion was measured by the phosphorescence quenching of preinfused Pd-porphyrin. The baseline arteriolar Po_2 (50–52 mmHg) decreased to about 5 mmHg for all the groups. Occlusion after HbV_8 infusion showed a slightly slower rate of Po_2 reduction compared with that after HbV_{29} infusion. The arteriolar O_2 content was calculated at each reducing Po_2 in combination with the O_2 equilibrium curves of HbVs, and it was clarified that HbV_8 showed a significantly slower rate of O_2 release compared with HbV_{29} and was a primary source of O_2 (maximum fraction, 0.55) overwhelming red blood cells when the Po_2 was reduced (e.g., <10 mmHg) despite a small dosage of HbV. This result supports the possible utilization of Hb-based O_2 carriers with lower P_{50} for oxygenation of ischemic tissues.

blood substitutes; artificial red blood cells; occlusion; microhemodynamics; liposome

PHOSPHOLIPID VESICLES encapsulating concentrated human Hb [Hb vesicles (HbV)] or liposome-encapsulated Hb can serve as a transfusion alternative whose O_2 carrying capacity can be formulated to be comparable to that of blood (1, 5, 8, 16, 24, 30). The capsular structure of HbV (particle diameter ~250 nm) has characteristics similar to those of natural red blood cells (RBCs), because both have membranes that prevent direct contact of Hb with the components of blood and the endothelial lining, mitigating cellular injury due to Hb-mediated prooxidative species (4, 38). Furthermore, Hb encapsulation in vesicles prevents a hypertensive response induced by free Hbs that scavenge the endogenous vasorelaxation factors nitric oxide (NO) and carbon monoxide (12, 18, 26). The safety of HbV has been confirmed in rodent models in terms of the prompt metabolism of the components of HbV in the reticuloendothelial system, which was demonstrated by histopathological analysis and plasma biochemical analysis (28, 29).

One of the characteristics of the capsular HbV is that its physicochemical characteristics such as O_2 affinity [O_2 tension at which Hb is half-saturated with O_2 (P_{50})] can be easily regulated by manipulating the amount of an allosteric effector coencapsulated in HbV. This property provides additional flexibility in formulating the O_2 transport properties of HbV by comparison with the chemically modified Hbs whose P_{50} is modified and fixed by chemical reactions such as cross-linking or polymer conjugation (34). We use pyridoxal 5′-phosphate (PLP) as the allosteric effector (33, 45). For example, coencapsulation of PLP at the molar ratio of PLP to Hb of 2.5:1 yields a P_{50} of about 29 mmHg. On the other hand, HbVs without PLP have a P_{50} of 8 mmHg. Historically, P_{50} was set similar to that of RBCs or about 25–30 mmHg, which theoretically allows sufficient O_2 unloading as blood transits the microcirculation. Decreasing O_2 affinity (increasing P_{50}) increases O_2 unloading in the peripheral blood circulation as shown by the enhanced O_2 release and improved exercise capacity in mutant mice that carry high P_{50} RBCs (36).

Hemoglobin-based O_2 carriers (HBOCs) of molecular dimensions as well as HbV could be effective for the targeted oxygenation of ischemic tissues (6, 43) because the small particle dimension would allow their passage through constricted or partially occluded vessels that do not allow the passage of RBCs (19). Blood flow in these vessels and in collateral vessels is usually slow, thus increasing RBC transit times (7, 11). As a result, tissue Po_2 is low and RBCs release most of their O_2 before reaching the capillary circulation. As an example, if tissue Po_2 is below 5 mmHg, O_2 saturation (Sa_{O_2}) of RBCs would be around 5%, and RBCs will have released most of their O_2 before they reach the ischemic tissue. Thus an HBOC with a normal P_{50} similar to RBCs would not be effective for carrying O_2 to the ischemic tissue.

In this study, we evaluate the rate of O_2 release from HbVs with high and low P_{50}s from arterioles immediately after their occlusion. We selected arterioles with diameters of about 50 μm because this size of arterioles contributes significantly to tissue oxygenation in normal conditions (13). This model was selected to determine the ability of HbVs to retain or release O_2 in hypoxic conditions and establish their suitability for oxygenating ischemic tissues.

Address for reprint requests and other correspondence: E. Tsuchida, Advanced Research Institute for Science and Engineering, Waseda Univ., Tokyo 169-8555, Japan (E-mail: eishun@waseda.jp).

The costs of publication of this article were defrayed in part by the payment of page charges. The article must therefore be hereby marked "*advertisement*" in accordance with 18 U.S.C. Section 1734 solely to indicate this fact.

MATERIALS AND METHODS

Preparation of HbVs. HbVs with different P_{50}s were prepared under sterile conditions as previously reported (32, 34, 37). Hb was purified from outdated donated human blood provided by the Japanese Red Cross Society (Tokyo, Japan). HbVs with a P_{50} = 29 mmHg (HbV_{29}) was prepared by adding the allosteric effector pyridoxal 5′-phosphate (PLP; 14.7 mM, Sigma Chemical; St. Louis, MO) to Hb (38 g/dl) at a molar ratio of PLP to Hb = 2.5. HbVs with a P_{50} = 8 mmHg (HbV_8) were prepared by adding no allosteric effector to the Hb solution. The Hb solution was encapsulated within vesicles composed of Presome PPG-I [a mixture of 1,2-dipalmitoyl-*sn*-glycero-3-phosphatidylcholine, cholesterol, and 1,5-di-*O*-octadecyl-*N*-succinyl-L-glutamate at a molar ratio of 5:5:1 (Nippon Fine Chemicals; Osaka, Japan)], and the particle size of HbVs was regulated by an extrusion method. The surface of the HbVs was modified with polyethylene glycol (molecular mass: 5 kDa, 0.3 mol% of the lipids in the outer surface of vesicles) using 1,2-distearoyl-*sn*-glycero-3-phosphatidylethanolamine-*N*-polyethylene glycol (Sunbright DSPE-50H, H-form, NOF; Tokyo, Japan). HbVs were suspended in a physiological salt solution and sterilized with filters (Dismic, Toyo Roshi; Tokyo, Japan; pore size: 0.45 μm) and deoxygenated with N_2 bubbling for storage. The endotoxin content was measured with a modified LAL
AQ: 1 assay, and the level was less than 0.2 EU/ml (27). The O_2 equilibrium curves (OECs) of HbV_{29} and HbV_8 were obtained by a Hemox Analyzer (TCS-Medical Products; Philadelphia, PA), as
F1 shown in Fig. 1. The physicochemical parameters of the HbVs are
T1 listed in Table 1.

Animal model and preparation. Experiments were carried out in 12 male Syrian golden hamsters (59 ± 12 g body wt, Charles Rivers; Worcester, MA). The dorsal skinfold consisting of two layers of skin and muscle was fitted with two titanium frames with a 15-mm circular opening and surgically installed under intraperitoneal pentobarbital sodium anesthesia (∼50 mg/kg body wt, Abbott Laboratory; North Chicago, IL). After the hair on the back skin of the hamster was removed, layers of skin muscle were separated from the subcutaneous tissue and removed until a thin monolayer of muscle including the small artery and vein and one layer of intact skin remained. A coverglass (diameter 12 mm) held by one frame covered the exposed tissue allowing intravital observation of the microcirculation (20, 22, 25).

Polyethylene (PE) tubes (PE-10, Becton-Dickinson; Parsippany, NJ; ∼1 cm) were connected to PE-50 tubing (∼25 cm) via silicone elastomer medical tubes (∼4 cm, Technical Products; Decatur, GA) and were implanted in the jugular vein and the carotid artery. They were passed from the ventral to the dorsal side of the neck and exteriorized through the skin at the base of the chamber. Patency of the catheters was ensured by filling them with heparinized saline (40

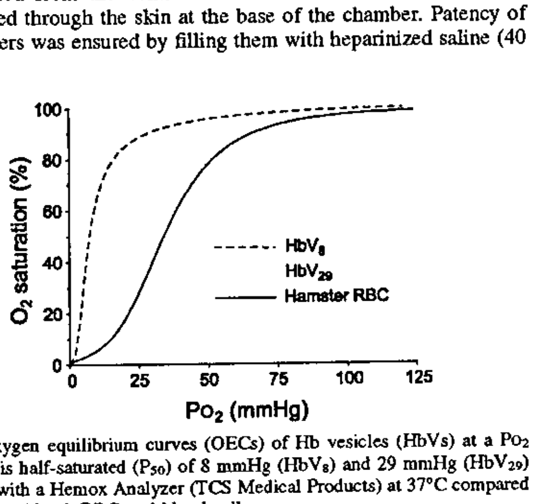

Fig. 1. Oxygen equilibrium curves (OECs) of Hb vesicles (HbVs) at a Po_2 where Hb is half-saturated (P_{50}) of 8 mmHg (HbV_8) and 29 mmHg (HbV_{29}) measured with a Hemox Analyzer (TCS Medical Products) at 37°C compared with hamster blood. RBC, red blood cells.

Table 1. *Physicochemical properties of HbV_8 and HbV_{29} compared with hamster blood*

Parameters	HbV_8	HbV_{29}	Hamster Blood
Hb concentration, g/dl	10	10	14.8 ± 0.5
Particle diameter, nm	250 ± 64	247 ± 44	5,000–7,000*
P_{50}, mmHg	8	29	28
Molar ratio of PLP to Hb	0	2.5	
MetHb, %	<3	<1	
HbCO, %	<2	<2	

HbV_8 and HbV_{29}, Hb vesicles (HbVs) at 8- and 29-mm Hg Po_2 at which Hb is 50% saturated (P_{50}); PLP, pyridoxal 5′-phosphate. *Size of hamster red blood cells (RBCs) (39).

IU/ml). Microvascular observations of the awake and unanesthetized hamsters were performed 5 days after chamber implantation to mitigate the effects of surgery. The hamster was placed in a perforated plastic tube from which the window chamber protruded to minimize animal movement without impeding respiration. All animal studies were approved by the Animal Care and Use Committee of University of California-San Diego and performed according to the National Institutes of Health *Guide for the Care and Use of Laboratory Animals* (Washington, DC: National Academy Press, 1996).

Infusion of HbV_8 and HbV_{29} and occlusion of an arteriole. The unanesthetized animal was placed in a perforated plastic tube and stabilized under the microscope. Animals were suitable for the experiments if systemic variables were within normal range, namely, heart rate >340 beats/min, mean arterial pressure >80 mmHg, systemic hematocrit >45%, and arterial Po_2 >50 mmHg, and microscopic examination of the tissue in the chamber did not reveal signs of edema or bleeding. Baseline measurements of microvascular parameters and Po_2 (see below) were performed before the infusion of HbV_8 or HbV_{29} suspended in physiological saline solution into the venous line at 7 ml/kg. Systemic blood volume was estimated as 70 ml/kg. In our previous reports of resuscitation from hemorrhagic shock or hemodilution, HbVs were suspended in an albumin solution to regulate colloid osmotic pressure (30, 33). However, in the present study, we did not use albumin to minimize the hypervolemic effect. For the same reason, the infusion amount was minimized to equal 10% blood volume (7 ml/kg).

After we stabilized the condition and measured the systemic parameters for 20 min, diameter and blood flow of the selected arterioles were measured. Large feeding arterioles or small arcading arterioles (diameter 53.0 ± 6.6 μm) were selected for observation. The arterioles were occluded by means of a glass micropipette whose end was drawn into a long fiber by a pipette puller (Fig. 2). The fiber F2
was bent over a flame, and the knee of the bend was used to press on the intact skin of the preparation mounted in an inverted microscope that allowed observation of the opposite side, i.e., the intact microcirculation. Once an arteriole was selected for measurement, the microoccluder is moved to the skin side, between the intact skin and the optics of the substage illumination. The tip of the occluder was placed near the center of the optical field of view of the microscope, and the vessel was similarly placed using the stage micrometric position control. This arrangement allowed for direct microscopic observation of the occluded vessel and the stopped flow as shown in Fig. 2. The duration of occlusion was 30 s.

Measurement of microhemodynamic parameters. Microvessels were observed by transillumination with an inverted microscope (IMT-2, Olympus; Tokyo, Japan). Microscopic images were video recorded (Cohu 4815-2000; San Diego, CA) and transferred to a television videocassette recorder (Sony Trinitron PVM-1271Q monitor; Tokyo, Japan) and Panasonic AG-7355 video recorder (Tokyo, Japan). Arterioles were classified according to their position within the microvascular network according to the previously reported scheme (33). Microvascular diameter and RBC velocity before occlu-

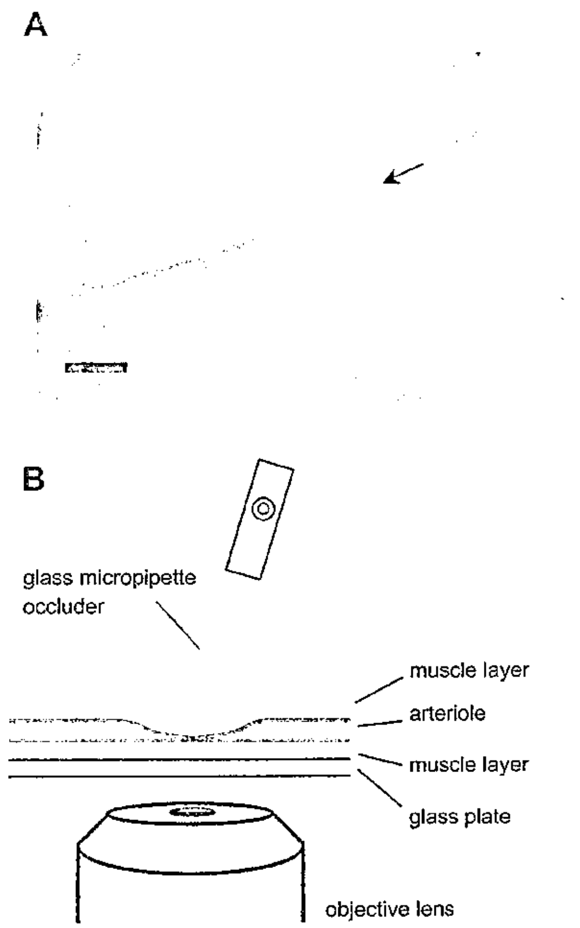

Fig. 2. *A*: microscopic image of an occluded arteriole in the hamster window chamber. The glass fiber lies across the arteriole. Scale bar = 100 μm. *B*: schematic representation of occlusion of *A* showing the different tissue layers of the skin (not to scale).

sion were analyzed on-line in the arterioles (14, 15). Vessel diameter was measured with an image-shearing system (Digital Video Image Shearing Monitor 908, I.P.M.; San Diego, CA), whereas RBC velocity was analyzed by photodiodes and the cross-correlation technique (Velocity Tracker Mod-102 B, I.P.M.). The blood flow rate (Q) was calculated using the following equation:

$$Q = (\text{RBC velocity}/R_v) \times (\text{diameter}/2)^2 \quad (1)$$

where R_v = 1.6 and is the ratio of the centerline velocity to average blood velocity according to data from glass tubes (20).

Palladium-porphyrin bound to bovine albumin solution (7.6 wt%, 0.1 ml) was injected intravenously 20 min before the infusion of HbVs. Arteriolar blood P_{O_2} was noninvasively determined by measuring the rate of decay of phosphorescence emitted by the metalloporphyrin complex after pulsed light excitation, which is a function of the local O_2 concentration (17, 40, 44). The relationship between phosphorescence lifetime and P_{O_2} is given by the following Stern-Volmer equation:

$$\tau_o/\tau = 1 + k_q \times \tau_o \times P_{O_2} \quad (2)$$

where τ_o and τ are the phosphorescence lifetimes in the absence of molecular O_2 and at a given P_{O_2}, respectively, and k_q is the quenching constant, with both factors being pH and temperature dependent. Light was gathered from an optical window of 20 × 5 μm placed longitudinally along the blood vessels. Measurements in the blood compartment were made every second using a single flash.

The P_{O_2} decay curves induced by the occlusion were obtained before the infusion of HbVs and 20 min after the infusion of HbVs. The Sa_{O_2} of HbVs at every P_{O_2} were obtained from the OECs (Fig. 1), and the total O_2 content in blood (ml O_2 in 1 dl blood) can be estimated using the following equation:

$$O_2\ \text{content} = 23.6 \times \frac{[Sa_{O_2}(\text{RBC}) + 0.0667 \times Sa_{O_2}(\text{HbV})]}{100} + 2.42 \times \frac{P_{O_2}}{713} \quad (3)$$

In this calculation, we used 15 g/dl as the average Hb concentration in arterial blood (14.8 ± 0.5 g/dl, heme concentration 9.3 mM), which was measured with a handheld photometer (B-Hemoglobin Photometer, Hemocue). One hundred milliliters of blood contain 23.6 ml O_2 bound to Hb when Sa_{O_2} is 100% (volume of an ideal gas at 37°C) according to Boyle-Charle's gas law, PV = *nRT*, where P (in atm) is atmospheric pressure, V (in liters) is gas volume, *n* is mole number, *R* is the gas constant (0.082 $atm \cdot l \cdot K^{-1} \cdot mol^{-1}$), and T is absolute temperature [23.6 (ml) = 9.3 × 10^{-4} (mol) × 0.082 × (273 + 37) × 1,000]. The physically dissolved O_2 content at 1 atm O_2 (713 mmHg after subtracting the vapor pressure of water = 47 mmHg) at 37°C was calculated to be 2.42 ml in 100 ml water. Sa_{O_2}(RBC) and Sa_{O_2}(HbV) are Sa_{O_2}s of RBCs and HbVs, respectively, at each arteriolar P_{O_2} during the experiments.

HbVs were suspended in physiological saline solution ([Hb] = 10 g/dl); therefore, their infusion lowered colloid osmotic pressure, causing the extravasation of plasma fluid. To account for this, we carried out our measurements 20 min after HbV infusion and assumed that this interval was sufficient for normalizing blood volume through the release of extra fluid to the interstitium, thus increasing plasma Hb concentration by 6.7%.

Data analysis. Data are given as means ± SD for the indicated number of animals. Data were analyzed using ANOVA followed by Fisher's protected least-significant difference test between groups according to the previous studies. Student's *t*-test was used for comparisons within each group. All statistics were calculated using GraphPad Prism 4.01 (Graph Pad Software; San Diego, CA). Changes were considered statistically significant if $P < 0.05$.

RESULTS

Hemodynamic properties of arterioles. The profiles of the selected arterioles, diameters, centerline RBC velocities, blood flow rates, and intra-arteriolar P_{O_2} values before and after infusion of HbVs are listed in Table 2. There was no significant T2
difference between the groups. The O_2 content in blood attributed to hamster RBCs and physically dissolved O_2 at the observed arteriolar P_{O_2} was estimated as 18.61 ± 1.23 ml O_2/dl blood according to *Eq. 3*. After the infusion of HbV_8 and HbV_{29}, the O_2 content increased to 20.30 ± 1.18 and 20.17 ± 1.54 ml O_2/dl blood, respectively, due to the O_2 bound to HbVs. The contributions of HbV_8 and HbV_{29} to whole O_2 content were 1.51 ± 0.01 and 1.25 ± 0.07 ml O_2/dl blood, respectively. The HbV_8 group showed higher O_2 content than the HbV_{29} group due to the higher $Sa_{O_2}(HbV_8)$, which was 95.9 ± 0.6% compared with the $Sa_{O_2}(HbV_{29})$ of 79.6 ± 4.7%.

Changes in P_{O_2} in arterioles after occlusion in the presence of HbVs. Arteriolar P_{O_2} before occlusion was about 50–52 mmHg in average for all groups and started to decrease significantly immediately after occlusion, as shown in Fig. 3. F3
In all groups, P_{O_2} fell to about 10 and 5 mmHg after 10- and

Table 2. *Profiles of arterioles for occlusion before and after infusion of HbVs*

Parameters	Before Infusion	After HbV Infusion	
		HbV_8	HbV_{29}
Arteriolar diameter, μm	53.0±6.6	56.2±6.8	55.8±6.9
Centerline flow velocity, mm/s	3.1±0.5	3.4±0.7	3.5±0.5
Blood flow rate, nl/s	6.8±1.6	8.7±3.1	8.5±2.1
Arteriolar Po_2, mmHg	50.7±4.7	51.4±4.8	52.1±5.3
Sa_{O_2}(RBC), %	78.1±5.1	76.0±7.7	77.9±6.5
Sa_{O_2}(HbV), %		95.9±0.6†	79.6±4.7
O_2 content in whole blood, ml/O_2/dl/blood	18.61±1.23	20.30±1.18*	20.17±1.54*
O_2 content in HbV, ml/O_2/dl/blood		1.51±0.01	1.25±0.07

Values are means ± SD. Arteriolar Po_2, O_2 saturation (Sa_{O_2}) and O_2 contents were obtained during 6 s before occlusion. *$P < 0.05$ vs. before infusion; †$P < 0.05$ vs. RBCs and HbV_{29}.

30-s occlusion, respectively. When the Po_2 values were expressed as relative to the baseline values (before occlusion), infusion of HbV_8 tended to show a slower rate of reduction of Po_2 compared with the infusion of HbV_{29} and without infusion (Fig. 4). There was a significant difference between the HbV_8 infusion and before infusion groups only at 7 s (P = 0.035). F4

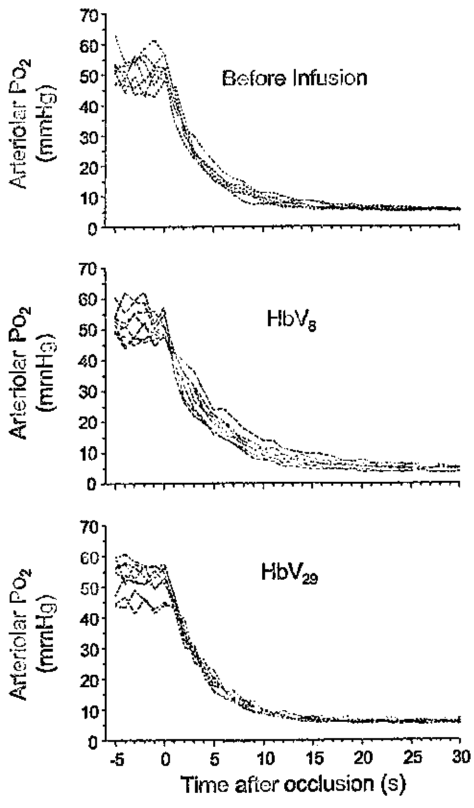

Fig. 3. Time course of Po_2 in the blood of an occluded arteriole (diameter, 53.0 ± 6.6 μm) before and after infusion of 7 ml/kg HbV_8 or HbV_{29} into hamsters. Measurements were made in blood at a distance of 50 μm from the point of occlusion. Most vessels equilibrate to intravascular partial pressure in the range of 4–6 mmHg about 15–20 s after occlusion.

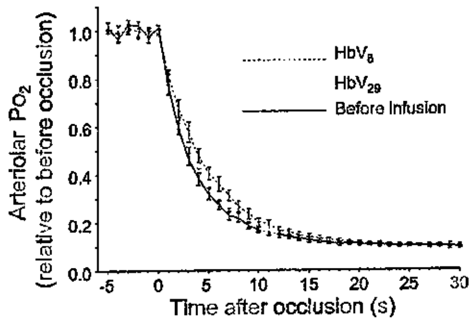

Fig. 4. Changes in Po_2 relative to before occlusion. The data in Fig. 3 were averaged. Baseline values before occlusion were obtained as the average of 6 values before occlusion and fixed as 1.0. There was a significant difference between the HbV_8 infusion and before infusion groups only at 7 s (P = 0.035).

Sa_{O_2}(RBC) and Sa_{O_2}(HbV) at every arteriolar Po_2 value can be estimated using the OECs in Fig. 1 assuming that the conditions in the arteriole (such as temperature and pH) do not change significantly from the normal condition (37°C, pH 7.4). Figure 5*A* shows the changes in the whole arteriolar O_2 content F5

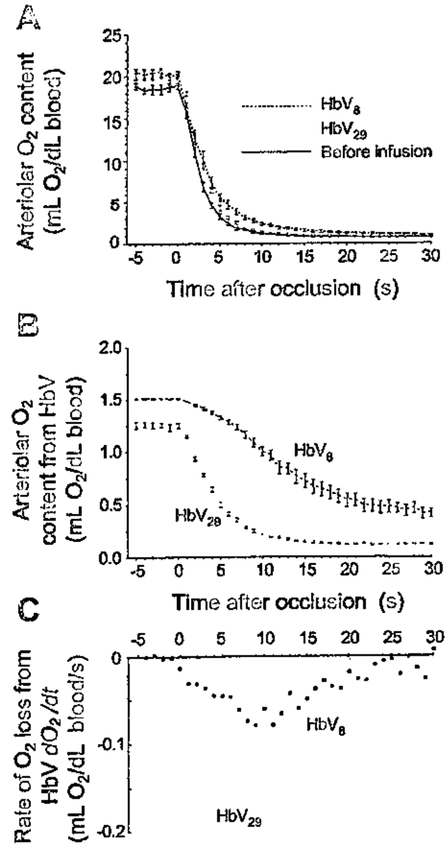

Fig. 5. *A*: time course of the arteriolar O_2 content in whole blood of an occluded arteriole before and after infusion of 7 ml/kg HbV_8 or HbV_{29} into hamsters. The O_2 contents were calculated using *Eq. 2* and the data of OECs (Fig. 1) and Po_2 changes (Fig. 3). *B*: time course of the O_2 content derived from HbVs in the blood. The contributions of HbVs are derived from the data in *A* and magnified in scale. *C*: rate of O_2 loss from HbVs. The graphs in *B* were differentiated and plotted.

during the occlusion. Immediately after occlusion, the O_2 content decreased rapidly. The HbV_8 group showed a slower rate of reduction compared with the HbV_{29} group and the group before HbV infusion. To demonstrate the contribution of HbVs clearly, only the O_2 content of HbVs is shown in Fig. 5*B*. HbV_8 showed a very slow rate of O_2 release. After 30 s of occlusion, the arteriolar Po_2 decreased to 5.2 ± 0.7 mmHg. However, $Sa_{O_2}(HbV_8)$ was 26.1 ± 7.3% and did not reach steady state but continued O_2 release. HbV_{29} showed almost no change after 15 s, and $Sa_{O_2}(HbV_{29})$ was 7.4 ± 1.0% after 30 s. Figure 5*C* shows the rate of O_2 loss from HbVs obtained by the differentiation of the graphs in Fig. 5B. HbV_{29} showed the fastest O_2 loss with the maximum of 0.18 ml O_2/dl blood sec after only 2 s of occlusion and did not supply O_2 after 17 s. On the other hand, HbV_8 showed a moderate O_2 loss and showed the maximum of 0.08 ml O_2/dl blood after 10 s of occlusion and continued to release O_2 until 30 s.

F6 Figure 6 shows the fraction of O_2 in blood originating from HbVs. Before occlusion of the arterioles, the fractions of HbV_8 and HbV_{29} are very small and similar because of the small dosage compared with the originally present RBCs. However, after occlusion, the fraction of O_2 from HbV_8 increased significantly and was about 0.55 after 10 s. This indicated that HbV_8, and not RBCs, was the main source of the O_2 carrier when Po_2 attained very low values.

DISCUSSION

The principal finding of this study is that HbV_8 (P_{50} = 8 mmHg) with a high O_2 affinity (low P_{50}) releases O_2 at a slower rate than does HbV_{29} in occluded arterioles of the hamster dorsal skinfold model. Furthermore, we found that HbV_8, and not HbV_{29}, is the main O_2 source in ischemic conditions.

The immediate occlusion of blood flow in the arterioles caused a rapid reduction of O_2 content. Similar phenomena have been observed by Richmond et al. (23) in rat spinotrapezius muscle tissue. There is substantial evidence that the arteriolar wall is a significant O_2 sink, consuming O_2 at a rate that is much greater than most tissues (9, 35, 42), which explains in part the significant and rapid drop of Po_2 found in our study. In our experiments, only one arteriole was occluded at a time in the intact subcutaneous tissue, and arteriolar Po_2 decreased to about 5 mmHg, which was higher than the critical Po_2 (2.9 ± 0.5 mmHg) in the rat spinotrapezius muscle tissue (23). Although the O_2 supply was significantly reduced, diffusion of O_2 from the other surrounding arterioles, venules, and capillaries near the occlusion should contribute to maintaining tissue Po_2 at a higher value than in the study of Richmond et al. (23), where the supply of blood to the tissue was stopped altogether. $Sa_{O_2}(HbV_8)$ at 5 mmHg is estimated to be about 26% according to the OECs (Fig. 1), which is higher than that for HbV_{29} (6%) and RBCs (2%); thus HbV_8 remains a source of O_2 for a longer period in a prolonged occlusion, because the fraction of O_2 from HbV_8 was 0.5 or higher, overwhelming the contribution from RBCs, as shown in Fig. 6.

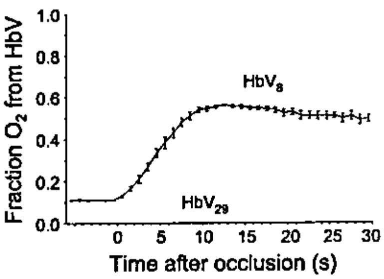

Fig. 6. Time course of the fraction of O_2 content from HbVs in whole blood. The extended time of occlusion induced hypoxic conditions and the fraction of O_2 content from HbV_8 increased significantly compared with HbV_{29}.

A limitation of our experimental method is that Sa_{O_2} is estimated under the assumption that conditions in the target arteriole are identical to that of the OEC measurement; however, the O_2 affinity of Hb changes as a function of temperature, pH, electrolyte concentration, and CO_2 content. Local ischemic conditions caused by the occlusion could affect pH and increase CO_2 tension, resulting in a slight decrease in the O_2 affinity (increased P_{50}); however, it is unlikely that this would introduce a significant error in the measurement of O_2 release considering the short duration of the occlusion (30 s).

We have previously demonstrated using an artificial narrow polymer tube (inner diameter: 28 μm) surrounded by a sodium dithionate solution to consume O_2 that a Hb solution under continuous flow conditions (1 mm/s) facilitates O_2 release when mixed with RBCs. Conversely, HbV did not show this phenomenon (31). This difference is due to the small size of O_2-bound acellular Hb molecules, which diffuse and therefore contribute to the facilitated O_2 transport (21, 31), whereas HbVs (diameter, about 250 nm) are too large to show sufficient diffusion for the facilitated O_2 transport. In these conditions, O_2 affinity (P_{50}) becomes the determining factor for the rate of O_2 release and transport to the vessels wall. Thus, in our present results, the presence of HbVs did not facilitate the reduction of Po_2 or O_2 content but retarded the reduction of Po_2 and O_2 content.

Our experimental model is designed to characterize the O_2 release behavior of blood from an occluded microvessel and does not directly related to clinical ischemic conditions because the occlusion of the small arteriole for 30 s does not induce tissue ischemia other than the transient event in the proximity of the microvessel. However, our data suggest that HbV_8 could be a significant source of O_2 in an ischemic condition with significantly lowered tissue Po_2. Because of the small dosage of HbV_8 (10 ml/kg), the O_2 content in the blood after occlusion (5 ml O_2/dl blood at 5 s) is significantly smaller than the baseline value (20 ml O_2/dl blood at 0 s). To enhance the contribution of HbVs, a larger dosage and sustained blood flow would be required. Contaldo et al. (7) recently demonstrated that inducing hemodilution using up to 50% blood exchange with HbV (P_{50} = 15 mmHg) suspended in dextran effectively oxygenated ischemic collaterized tissue in skin flaps. This phenomenon could be explained by low P_{50} HbVs retaining O_2 in the upstream vessels and delivering it to the ischemic tissue via collateral arterioles, even when these may have significantly slower blood flow. It has been proposed that small-sized HBOCs oxygenate ischemic tissue by being able to pass through constricted or partially occluded vessels that do not allow the passage of RBCs; however, the results from Contaldo et al. (17) as well as those from our experimental model do not serve to support this concept, because arterioles were completely ligated or occluded. It should be noted, however, that an advantage of small HBOCs, including HbVs, is that they are homogeneously dispersed in the plasma phase and therefore can deliver O_2 more homogeneously to the periphery than RBCs because microvascular hematocrit is heterogeneous particularly in pathological states. In such conditions, HbVs with a higher O_2 affinity should show a slower O_2 unloading that would be effective for oxygenating ischemic tissues.

In conclusion, HbVs provide the unique feature of allowing for the regulation of P_{50} by modulating the amount of coencapsulated PLP (33, 45). Recent studies showed the effectiveness of HBOCs with a lower P_{50} (higher O_2 affinity) as a means of implementing O_2 delivery targeted to ischemic tissue (2, 3, 41, 43). Thus this experimental method provides data useful for the design and optimization of O_2 carriers and suggests the possible utilization of HbVs for therapeutic approaches aimed at remedying ischemic conditions.

ACKNOWLEDGMENTS

The authors greatly acknowledge A. Barra and C. Walser (University of California-San Diego) for help with the animal preparations, Dr. S. Takeoka and Dr. K. Sou (Waseda University) for the preparation of the HbVs, and Dr. D. Erni (Inselspital University Hospital, Bern, ~~Germany~~ Switzerland) for meaningful discussions.

GRANTS

This study was supported in part by Health Sciences Research grants (Regulatory Science, Artificial Blood Project); the Ministry of Health, Labour and Welfare, Japan; Japan Society for the Promotion of Science Grant-In-Aid for Scientific Research B16300162; and National Heart, Lung, and Blood Institute Bioengineering Partnership Grant R24 HL-64395 and Grants R01 HL-40696 and R01 HL-62354. H. Sakai was an overseas research fellow of the Society of Japanese Pharmacopoeia.

REFERENCES

1. **Awasthi VD, Garcia D, Klipper R, Goins BA, and Phillips WT.** Neutral and anionic liposome-encapsulated hemoglobin: effect of postinserted poly(ethylene glycol)-distearoylphosphatidylethanolamine on distribution and circulation kinetics. *J Pharmacol Exp Ther* 309: 241–248, 2004.
2. **Baines AD, Adamson G, Wojciechowski P, Pliura D, Ho P, and Kluger R.** Effect of modifying O_2 diffusivity and delivery on glomerular and tubular function in hypoxic perfused kidney. *Am J Physiol Renal Physiol* 274: F744–F752, 1998.
3. **Baines AD and Ho P.** O_2 affinity of cross-linked hemoglobins modifies O_2 metabolism in proximal tubules. *J Appl Physiol* 95: 563–570, 2003.
4. **Buehler PW and Alayash AI.** Toxicities of hemoglobin solutions: in search of in-vitro and in-vivo model systems. *Transfusion* 44: 1516–1530, 2004.
5. **Chang TMS.** *Blood Substitutes: Principles, Methods, Products, and Clinical Trials.* Basel: Karger, 1997.
6. **Cabrales P, Sakai H, Tsai AG, Tsuchida E, and Intaglietta M.** Oxygen transport by low and normal P_{50} hemoglobin vesicles in extreme hemodilution. *Am J Physiol Heart Circ Physiol* 288: H1885–H1892, 2005. First published November 24, 2004; doi:10.1152/ajpheart.01004.2004.
7. **Contaldo C, Schramm S, Wettstein R, Sakai H, Takeoka S, Tsuchida E, Leunig M, Banic A, and Erni D.** Improved oxygenation in ischemic hamster flap tissue is correlated with increasing hemodilution with Hb vesicles and their O_2 affinity. *Am J Physiol Heart Circ Physiol* 285: H1140–H1147, 2003.
8. **Djordjevich L, Mayoral J, Miller IF, and Ivankovich AD.** Cardiorespiratory effects of exchange transfusions with synthetic erythrocytes in rats. *Crit Care Med* 15: 318–323, 1987.
9. **Duling BR and Berne RM.** Longitudinal gradients in periarteriolar oxygen tension. A possible mechanism for the participation of oxygen in the local regulation of blood flow. *Circ Res* 27: 669–678, 1970.
10. **Endrich B, Asaishi K, Gotz A, and Messmer K.** Technical report: a new chamber technique for microvascular studies inunanesthetized hamsters. *Res Exp Med (Berl)* 177: 125–134, 1980.
11. **Erni D, Wettstein R, Schramm S, Sakai H, Takeoka S, Tsuchida E, Leunig M, and Banic A.** Normovolemic hemodilution with hemoglobin-vesicle solution attenuates hypoxia in ischemic hamster flap tissue. *Am J Physiol Heart Circ Physiol* 284: H1702–H1709, 2003.
12. **Goda N, Suzuki K, Naito S, Takeoka S, Tsuchida E, Ishimura Y, Tamatani T, and Suematsu M.** Distribution of heme oxygenase isoform in rat liver: topographic basis for carbon monoxide-mediated micorvascular relaxation. *J Clin Invest* 101: 604–612, 1998.
13. **Intaglietta M, Johnson PC, and Winslow RM.** Microvascular and tissue oxygen distribution. *Cardiovasc Res* 32: 632–643, 1996.
14. **Intaglietta M, Silverman NR, and Tompkins WR.** Capillary flow velocity measurements in vivo and in situ by television methods. *Microvasc Res* 10: 165–179, 1975.
15. **Intaglietta M and Tompkins WR.** Microvascular measurements by video image shearing and splitting. *Microvasc Res* 5: 309–312, 1973.
16. **Izumi Y, Sakai H, Hamada K, Takeoka S, Yamahata Y, Kato R, Nishide H, Tsuchida E, and Kobayashi K.** Physiologic responses to exchange transfusion with hemoglobin vesicles as an artificial oxygen carrier in anesthetized rats: changes in mean arterial pressure and renal cortical tissue oxygen tension. *Crit Care Med* 24: 1869–1873, 1996.
17. **Kerger H, Torres Filho IP, Rivas M, Winslow RM, and Intaglietta M.** Systemic and subcutaneous microvascular oxygen tension in conscious Syrian golden hamsters. *Am J Physiol Heart Circ Physiol* 268: H802–H810, 1995.
18. **Kyokane Norimuzu S T, Taniai H, Yamaguchi T, Takeoka S, Tsuchida E, Naito M, Nimura Y, Ishimura Y, and Suematsu M.** Carbon monoxide from heme catabolism protects against hepatobiliary dysfunction in endotoxin-treated rat liver. *Gastroenterology* 120: 1227–1240, 2001.
19. **Linberg R, Conover CD, Shum KL, and Shorr RGL.** Increased tissue oxygenation and enhanced radiation sensitivity of solid tumors in rodents following polyethylene glycol conjugated bovine hemoglobin administration. In Vivo 12: 167–174, 1998.
20. **Lipowsky HH and Zweifach B.** Application of the "two slit" photometric technique to the measurement of microvascular volumetric flow rates. *Microvasc Res* 15: 93–101, 1978.
21. **McCarthy MR, Vandegeriff KD, and Winslow RM.** The role of facilitated diffusion in oxygen transport by cell-free hemoglobins: implications for the design of hemoglobin-based oxygen carriers. *Biophys Chem* 92: 103–117, 2001.
22. **Papenfuss HD, Gross JF, Intaglietta M, and Treese FA.** A transparent access chamber for the rat dorsal skin fold. *Microvasc Res* 18: 311–318, 1979.
23. **Richmond KN, Shonat RD, Lynch RM, and Johnson PC.** Critical Po_2 of skeletal muscle in vivo. *Am J Physiol Heart Circ Physiol* 277: H1831–H1840, 1999.
24. **Rudolph AS, Klipper RW, Goins B, and Phillips WT.** In vivo biodistribution of a radiolabelled blood substitute: ^{99m}Tc-labeled liposome-encapsulated hemoglobin in an anesthetized rabbit. *Proc Natl Acad Sci USA* 88: 10976–10980, 1991.
25. **Sakai H, Hara H, Tsai AG, Tsuchida E, Johnson PC, and Intaglietta M.** Changes in resistance vessels during hemorrhagic shock and resuscitation in conscious hamster model. *Am J Physiol Heart Circ Physiol* 276: H563–H571, 1999.
26. **Sakai H, Hara H, Yuasa M, Tsai AG, Takeoka S, Tsuchida E, and Intaglietta M.** Molecular dimensions of Hb-based O_2 carriers determine constriction of resistance arteries and hypertension in conscious hamster model. *Am J Physiol Heart Circ Physiol* 279: H908–H915, 2000.
27. **Sakai H, Hisamoto S, Fukutomi I, Sou K, Takeoka S, and Tsuchida E.** Detection of lipopolysaccharide in hemoglobin-vesicles by *Limulus amebocyte* lysate test with kinetic-turbidimetric gell clotting analysis and pretreatment with a surfactant. *J Pharm Sci* 93: 310–321, 2004.
28. **Sakai H, Horinouchi H, Tomiyama K, Ikeda E, Takeoka S, Kobayashi K, and Tsuchida E.** Hemoglobin-vesicles as oxygen carriers: influence on phagocytic activity and histopathological changes in reticuloendothelial systems. *Am J Pathol* 159: 1079–1088, 2001.
29. **Sakai H, Masada Y, Horinouchi H, Ikeda E, Sou K, Takeoka S, Suematsu M, Kobayashi K, and Tsuchida E.** Physiologic capacity of reticuloendothelial system for degradation of hemoglobin-vesicles (artificial oxygen carriers) after massive intravenous doses by daily repeated infusion for 14 days. *J Pharmacol Exp Ther* 311: 874–884, 2004.
30. **Sakai H, Masada Y, Horinouchi H, Yamamoto M, Ikeda E, Takeoka S, Kobayashi K, and Tsuchida E.** Hemoglobin-vesicles suspended in recombinant human serum albumin for resuscitation from hemorrhagic shock in anesthetized rats. *Crit Care Med* 32: 539–545, 2004.

31. **Sakai H, Suzuki Y, Kinoshita M, Takeoka S, Maeda N, and Tsuchida E.** O_2-release from Hb-vesicles evaluated using an artificial narrow O_2-permeable tube: comparison with RBC and acellular Hb. *Am J Physiol Heart Circ Physiol* 285: H2543–H2551, 2003.
32. **Sakai H, Takeoka S, Yokohama H, Seino Y, Nishide H, and Tsuchida E.** Purification of concentrated Hb using organic solvent and heat treatment. *Protein Expr Purif* 4: 563–569, 1993.
33. **Sakai H, Tsai AG, Rohlfs RJ, Hara H, Takeoka S, Tsuchida E, and Intaglietta M.** Microvascular responses to hemodilution with Hb-vesicles as red blood cell substitutes: influences of O_2 affinity. *Am J Physiol Heart Circ Physiol* 276: H553–H562, 1999.
34. **Sakai H, Yuasa M, Onuma H, Takeoka S, and Tsuchida E.** Synthesis and physicochemical characterization of a series of hemoglobin-based oxygen carriers: objective comparison between cellular and acellular types. *Bioconjug Chem* 11: 56–64, 2000.
35. **Shibata M, Ichioka S, Ando J, and Kamiya A.** Microvascular and interstitial P_{O_2} measurements in rat skeletal muscle by phosphorescence quenching. *J Appl Physiol* 91: 321–327, 2001.
36. **Shirasawa T, Izumizaki M, Suzuki YI, Ishihara A, Shimizu T, Tamaki M, Huang F, Koizumi KI, Iwase M, Sakai H, Tsuchida E, Ueshima U, Inoue H, Koseki H, Senda H, Kuriyama T, and Homma I.** Oxygen affinity of hemoglobin regulates O_2 consumption, metabolism, and physical activity. *J Biol Chem* 278: 5035–5043, 2003.
37. **Sou K, Naito Y, Endo T, Takeoka S, and Tsuchida E.** Effective encapsulation of proteins into size-controlled phospholipid vesicles using freeze-thawing and extrusion. *Biotechnol Progr* 19: 1547–1552, 2003.
38. **Takeoka S, Teramura Y, Atoji T, and Tsuchida E.** Effect of Hb-encapsulation with vesicles on H_2O_2 reaction and lipid peroxidation. *Bioconjug Chem* 13: 1302–1308, 2002.
39. **Tomson FN and Wardrop KJ.** Clinical chemistry and hematology. In: *Laboratory Hamsters*, edited by van Hoosier GL Jr and McPherson CW. Orlando, FL: Academic, 1987, chapt. 3. AQ: 2
40. **Torres Filho IP and Intaglietta M.** Microvascular P_{O_2} measurements by phosphorescence decay method. *Am J Physiol Heart Circ Physiol* 265: H1434–H1438, 1993.
41. **Tsai AG, Kerger H, and Intaglietta M.** Microcirculatory consequences of blood substitutution with αα-hemoglobin. In: *Blood Substitutes: Physiological Basis of Efficacy*, edited by Winslow RM, Vandegriff K, and Intaglietta M. Boston, MA: Birkhauser, 1995, p. 155–174.
42. **Tsai AG, Friesenecker B, Mazzoni MC, Kerger H, Buerk DG, Johnson PC, and Intaglietta M.** Microvascular and tissue oxygen gradients in the rat mesentery. *Proc Natl Acad Sci USA* 95: 6590–6595, 1998.
43. **Tsai AG, Vandegriff KD, Intaglietta M, and Winslow RM.** Targeted O_2 delivery by low-P_{50} hemoglobin: a new basis for O_2 therapeutics. *Am J Physiol Heart Circ Physiol* 285: H1411–H1419, 2003.
44. **Vanderkooi JM, Maniara G, Green TJ, and Wilson DF.** An optical method for measurement of dioxygen concentration based on quenching of phosphorescence. *J Biol Chem* 262: 5476–5482, 1987.
45. **Wang L, Morizawa K, Tokuyama S, Satoh T, and Tsuchida E.** Modulation of oxygen-carrying capacity of artificial red cells (ARC). *Polymer Adv Technol* 4: 8–11, 1992.

Am J Physiol Heart Circ Physiol 288: H1885–H1892, 2005.
First published November 24, 2004; doi:10.1152/ajpheart.01004.2004.

Oxygen transport by low and normal oxygen affinity hemoglobin vesicles in extreme hemodilution

Pedro Cabrales,[1,2] Hiromi Sakai,[3] Amy G. Tsai,[1,2] Shinji Takeoka,[3] Eishun Tsuchida,[3] and Marcos Intaglietta[1,2]

[1]*Department of Bioengineering, University of California-San Diego, and* [2]*La Jolla Bioengineering Institute, La Jolla, California; and* [3]*Advanced Research Institute for Science and Engineering, Waseda University, Tokyo, Japan*

Submitted 1 October 2004; accepted in final form 18 November 2004

Cabrales, Pedro, Hiromi Sakai, Amy G. Tsai, Shinji Takeoka, Eishun Tsuchida, and Marcos Intaglietta. Oxygen transport by low and normal oxygen affinity hemoglobin vesicles in extreme hemodilution. *Am J Physiol Heart Circ Physiol* 288: H1885–H1892, 2005. First published November 24, 2004; doi:10.1152/ajpheart.01004.2004.—The oxygen transport capacity of phospholipid vesicles encapsulating purified Hb (HbV) produced with a Po_2 at which Hb is 50% saturated (P_{50}) of 8 (HbV_8) and 29 mmHg (HbV_{29}) was investigated in the hamster chamber window model by using microvascular measurements to determine oxygen delivery during extreme hemodilution. Two isovolemic hemodilution steps were performed with 5% recombinant albumin (rHSA) until Hct was 35% of baseline. Isovolemic exchange was continued using HbV suspended in rHSA solution to a total [Hb] of 5.7 g/dl in blood. P_{50} was modified by coencapsulating pyridoxal 5′-phosphate. Final Hct was 11% for the HbV groups, with a plasma [Hb] of 2.1 ± 0.1 g/dl after exchange with HbV_8 or HbV_{29}. A reference group was hemodiluted to Hct 11% with only rHSA. All groups showed stable blood pressure and heart rate. Arterial oxygen tensions were significantly higher than baseline for the HbV groups and the rHSA group and significantly lower for the HbV groups compared with the rHSA group. Blood pressure was significantly higher for the HbV_8 group compared with the HbV_{29} group. Arteriolar and venular blood flows were significantly higher than baseline for the HbV groups. Microvascular oxygen delivery and extraction were similar for the HbV groups but lower for the rHSA group ($P < 0.05$). Venular and tissue Po_2 were statistically higher for the HbV_8 vs. the HbV_{29} and rHSA groups ($P < 0.05$). Improved tissue Po_2 is obtained when red blood cells deliver oxygen in combination with a high- rather than low-affinity oxygen carrier.

oxygen-carrying capacity; blood substitutes; tissue oxygen; hemoglobin oxygen affinity

PHOSPHOLIPID VESICLES encapsulating concentrated hemoglobin (Hb) solution [Hb vesicles (HbV) or liposome-encapsulated Hb] provide oxygen-carrying capacity to plasma expanders, reproducing several of the characteristics of red blood cells (RBC) suspended in plasma. HbV contain Hb at a high concentration within a cell membrane-like structure. Their oxygen dissociation curve can be adjusted by varying the concentration of pyridoxal 5′-phosphate (PLP). A widely accepted premise for designing a blood substitute is that its Hb should have an oxygen dissociation curve like that of RBC or one that is right shifted, i.e., having a high P_{50} to facilitate the unloading of oxygen (P_{50} is the partial pressure of oxygen at which the Hb molecule is 50% saturated). In a previous study by Sakai et al. (16), vesicles were formulated with P_{50} values set at 9, 16, and 30 mmHg. The study showed that optimal tissue oxygen conditions were obtained when 80% of the circulating blood was substituted with HbV whose P_{50} was 16 mmHg, a value considerably lower than the usual value of 28 mmHg for normal blood (16). Oxygen-carrying capacity was found to be well above the oxygen supply limitation.

Recent developments in the field of oxygen-carrying plasma expanders (OCPE) based on molecular Hb solutions reported by Tsai et al. (22) show that the addition of comparatively small amounts of a significantly left-shifted polyethylene glycol-conjugated oxygen carrier (P_{50} ~5 mmHg) to blood in extreme hemodilution leads to baseline microvascular and systemic conditions. This result could not be obtained in identical extreme hemodilution experiments with the use of a right-shifted molecular Hb solution at a considerably higher concentration (19).

Extreme hemodilution in the hamster window chamber model to a hematocrit (Hct) level of ~11% is a powerful tool to test the efficacy of OCPEs in restoring microvascular function and systemic conditions. This Hct is below the threshold at which the organism becomes oxygen supply limited (5, 22, 23). In this scenario, the effects of a blood substitute became magnified upon introduction into the circulation. Furthermore, by encapsulating Hb, a phospholipid vesicle eliminates the problem of Hb extravasation and provides a setting in which the biophysical properties of the infusion solution can be rigorously controlled while allowing for the change in P_{50}. Therefore, experimenting with vesicles that encapsulate Hb formulated with different P_{50} values provides the unique opportunity to investigate how oxygen affinity regulates oxygen delivery to the tissue by the microcirculation, a value not attainable by lowering RBC Hb P_{50} by the administration of sodium cyanate, which may introduce changes in tissue metabolism (7). In addition, RBC and HbV are different in size, flow pattern, homogeneous distribution in the plasma phase, and the mechanism of oxygen unloading in capillaries, and direct comparison between RBC and HbV is impossible. All these conditions indicate that the optimal P_{50} should be different in HbV and RBC.

In the present study, we investigated the microvascular effects of restoring oxygen-carrying capacity in conditions of extreme hemodilution, introducing by exchange transfusion identical amounts of Hb-carrying vesicles in which oxygen affinity was specifically controlled so that P_{50} was either 8 or 29 mmHg. The P_{50} value of 8 mmHg was chosen because it is

Address for reprint requests and other correspondence: P. Cabrales, Dept. of Bioengineering, 0412, 9500 Gilman Dr., Univ. of California-San Diego, La Jolla, CA 92093-0412 (E-mail: pcabrales@ucsd.edu).

The costs of publication of this article were defrayed in part by the payment of page charges. The article must therefore be hereby marked "*advertisement*" in accordance with 18 U.S.C. Section 1734 solely to indicate this fact.

similar to that of a recently developed oxygen carrier that is effective at a low concentration (2–4, 22). In these experiments, the hemodilution protocols were performed using a recombinant albumin solution (13) as the plasma expander.

METHODS

Investigations were performed in male golden Syrian hamsters (55–65 g body wt) fitted with a dorsal skinfold chamber window (6). This model has been used extensively for investigations of the intact microvasculature of adipose and subcutaneous tissue and skeletal muscle in conscious animals for extended periods. Pentobarbital sodium (50 mg/kg ip) was used for window implantation and for carotid artery and jugular vein catheterization. The microvasculature was examined 4–5 days after the initial surgery, and only animals passing an established systemic and microcirculatory inclusion criteria, which included having tissue void of low perfusion, inflammation, and edema (21), were entered into the study. Animal handling and care followed the NIH *Guide for the Care and Use of Laboratory Animals*. The experimental protocol was approved by the local animal care committee.

Preparation of HbV with different P_{50}. HbV were prepared under sterile conditions as previously reported (12, 15). Hb was purified from outdated donated blood provided by the Hokkaido Red Cross Blood Center (Sapporo, Japan) and the Japanese Red Cross Society (Tokyo, Japan). The encapsulated purified Hb (38 g/dl) contained 0 or 14.7 mM PLP (Sigma Chemical, St. Louis, MO) as an allosteric effector at a molar ratio of [PLP]/[Hb] = 0 or 2.5, respectively. The lipid bilayer was composed of a mixture of 1,2-dipalmitoyl-*sn*-glycero-3-phosphatidylcholine, cholesterol, and 1,5-bis-*O*-hexadecyl-*N*-succinyl-L-glutamate at a molar ratio of 5:5:1 (Nippon Fine Chemical, Osaka, Japan) and 1,2-distearoyl-*sn*-glycero-3-phosphatidylethanolamine-*N*-poly(ethylene glycol) (0.3 mol% of the total lipid; NOF, Tokyo, Japan) (17). HbV with a 250-nm diameter were suspended in a physiological saline solution in which [Hb] = 10 g/dl, sterilized with filters (Dismic, pore size 0.45 μm; Toyo Roshi, Tokyo, Japan), and deoxygenated with N_2 bubbling for storage (14). The content of lipopolysaccharide was <0.1 EU/ml.

Before use, the HbV suspension ([Hb] = 10 g/dl, 8.6 ml) was mixed with a solution of recombinant human serum albumin (rHSA 25%, 1.4 ml; Nipro, Osaka, Japan) to regulate the rHSA concentration in the suspending medium of the vesicles to 5 g/dl. Under this condition, the colloid osmotic pressure of the suspension is ~20 mmHg (Wescor 4420 colloid osmometer; Wescor, Logan, UT) (12). As a result, the Hb concentration of the suspension was 8.6 g/dl.

In a previous study (16), HbV were suspended in 8 g/dl HSA. However, we changed to 5 g/dl rHSA because it showed better microvascular perfusion in the hamster window model (i.e., increased red cell velocity and functional capillary density) than 8 g/dl HSA. The suspension was filtered through sterile filters (pore size 0.45 μm; Millipore, Billerica, MA). The characteristics of HbV are listed in Table 1, with all parameters being almost identical except oxygen affinity (HbV_8, P_{50} = 8 mmHg; HbV_{29}, P_{50} = 29 mmHg).

Table 1. *Physical characteristics of solutions*

Fluid	Viscosity, cp	COP, mmHg	P_{50}, mmHg
rHSA (5%)	0.98	20	
HbV_8 (10 g Hb/dl)	2.92		8
HbV_{29} (10 g Hb/dl)	2.96		29
HbV_8/rHSA (8.6 g Hb/dl)	2.87	20	8
HbV_{29}/rHSA (8.6 g Hb/dl)	2.90	20	29

Viscosity was measured at a shear rate of 160 s^{-1} at 37°C. COP, colloid osmotic pressure measured at 27°C; P_{50}, partial pressure of oxygen at which Hb is 50% saturated; rHSA, recombinant human serum albumin; HbV_8 and HbV_{29}, Hb vesicles with a P_{50} of 8 and 29 mmHg, respectively.

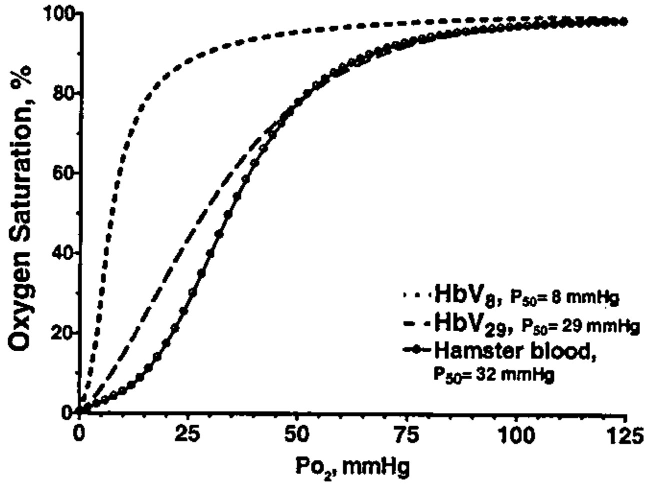

Fig. 1. Oxygen dissociation curves for phospholipid vesicles encapsulating purified Hb (HbV) produced with a Po_2 at which Hb is 50% saturated (P_{50}) of 8 (HbV_8) and 29 mmHg (HbV_{29}) vs. the dissociation curve for hamster blood (P_{50} = 32 mmHg).

Measurements of P_{50} and rate of oxygen release from HbV. The P_{50} and Hill number of each HbV and Hb solution were calculated from oxygen dissociation curves measured with a Hemox analyzer (TCS-Medical Products) at 37°C (Fig. 1).

Acute isovolemic exchange-transfusion (hemodilution) protocol. Progressive hemodilution to a final systemic Hct level of 11% was accomplished with three isovolemic exchange steps. This protocol, leading to extreme hemodilution while maintaining stable hemodynamic conditions, is described in detail in a previous report by Tsai (19). Briefly, the volume of each exchange-transfusion step was calculated as a percentage of the blood volume, estimated as 7% of the body weight. An acute anemic state was induced by lowering systemic Hct by 60% with two steps of progressive isovolemic hemodilution using 5% rHSA, referred to as exchange *levels 1* and *2*. *Level 1* exchange was 40% of blood volume, and *level 2* and *3* exchanges were 35% of blood volume, respectively.

After *level 2*, the animals were randomly divided into three experimental groups by being assigned to an experimental group according to a sorting scheme based on a list of random numbers (1). *Level 2* exchange was followed by *level 3* exchange. Hemodilution with 5% rHSA solution was continued with one group of the *level 2* hemodiluted animals, the experimental group rHSA, until Hct was decreased to 11% of baseline (Fig. 2). The test materials were studied by assigning the remainder of the *level 2* animals to groups labeled HbV_8 (P_{50} = 8 mmHg) and HbV_{29} (P_{50} = 29 mmHg) and were hemodiluted using these materials, reducing Hct to 11%. Plasma Hb concentrations derived for HbV_8 and HbV_{29} after exchange of 35% blood volume are estimated around 2.0–2.3 g/dl for both groups (35% of estimated total Hb content) (21).

Because mixed blood is withdrawn during the exchanges, a 110% blood volume exchange was needed to reduce Hct to 25% of baseline (11% Hct). Test solutions were infused into the jugular vein catheter after passing through an in-line, 13-mm-diameter, 0.2-μm syringe filter at a rate of 100 μl/min. Blood was simultaneously withdrawn using a dual syringe pump ("33" syringe pump; Harvard Apparatus, Holliston, MA) at the same (isovolemic-normovolemic) rate from the carotid artery catheter (4, 5, 19). This slow rate of exchange provided for a stable mean arterial pressure immediately after the exchange. Each animal was allowed a 10-min stabilization period before data acquisition.

Blood chemistry and biophysical properties. Arterial blood was collected in heparinized glass capillaries (0.05 ml) and immediately

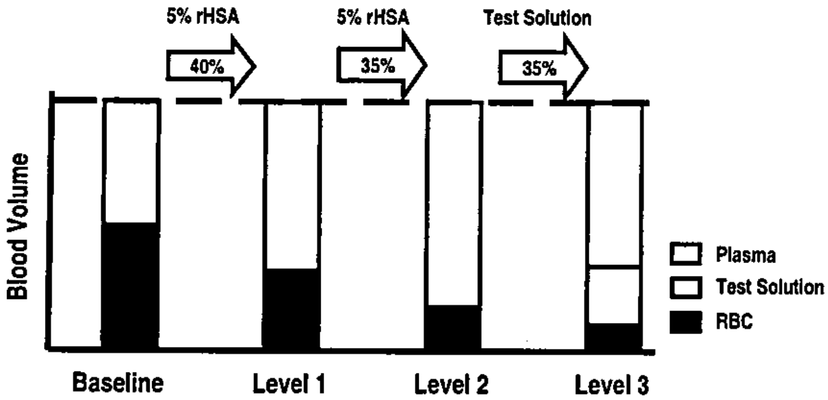

Fig. 2. Hemodilution was attained by means of a progressive, stepwise, isovolemic blood exchange-transfusion protocol. Volume of each exchange-transfusion step was calculated as a percentage of the blood volume, estimated as 7% of body weight. An acute anemic state was induced by lowering systemic Hct, using a 5% recombinant human serum albumin (rHSA) solution, in 2 progressive steps of isovolemic hemodilution labeled *level 1* and *level 2* exchanges. *Level 3* exchange was achieved by a third hemodilution that continued using rHSA or the vesicle solutions HbV_8 or HbV_{29} suspended in 5% rHSA (test solutions). RBC, red blood cells.

analyzed for arterial P_{O_2} (Pa_{O_2}), arterial P_{CO_2} (Pa_{CO_2}), base excess (BE), and pH (Blood Chemistry Analyzer 248; Bayer, Norwood, MA). The comparatively low Pa_{O_2} and high Pa_{CO_2} values of these animals is a consequence of their adaptation to a fossorial environment. Blood samples for viscosity and colloid osmotic pressure measurements were quickly withdrawn from the animal with a heparinized 5-ml syringe at the end of the experiment for immediate analysis.

Viscosity was measured in a cone/plate viscometer (DV-II+) with a cone spindle (CPE-40; both from Brookfield Engineering Laboratories, Middleboro, MA) at a shear rate of 160 s^{-1}. Colloid osmotic pressure (COP) was measured using the Wescor 4420 colloid osmometer (23).

Functional capillary density. Functional capillary density (FCD; in cm^{-1}) is the total length of RBC-perfused capillaries divided by the area of the microscopic field of view (21). Capillary segments were considered functional if RBC were observed to transit over a 30-s period. FCD was tabulated from the capillary lengths with RBC flow in an area comprising 10 successive microscopic fields (420 × 320 μm). Detailed mappings were made of the chamber vasculature to study the same microvessels throughout the experiment.

Microhemodynamic parameters. Arteriolar and venular blood flow velocities were measured online using the photodiode cross-correlation technique (8) (Fiber Optic Photo Diode and Velocity Tracker Correlator model 102B; Vista Electronics, Ramona, CA). The centerline velocity (*V*) was corrected according to vessel size to obtain the mean RBC velocity (11). The video image shearing technique was used to measure vessel diameter (*D*) online. Blood flow was calculated from the measured parameters as (Q) = $V\pi(D/2)^2$.

Microvascular P_{O_2} distribution. High-resolution microvascular P_{O_2} measurements were made using phosphorescence-quenching microscopy (18), a method based on the oxygen-dependent quenching of phosphorescence emitted by albumin-bound metalloporphyrin complex after pulsed light excitation. Phosphorescence microscopy is not dependent on the level of dye within the tissue, and the decay time is inversely proportional to the P_{O_2} level. The phosphorescence decay curves were converted to oxygen tensions by using a fluorescence decay curve fitter (model 802; Vista Electronics) (9). This technique has been used in this animal preparation and others for both intravascular and extravascular oxygen tension measurements, because albumin exchange between plasma and tissue allows for sufficient concentrations of albumin-bound dye within the interstitium to achieve an adequate signal-to-noise ratio. Animals received a slow intravenous injection of 15 mg/kg body wt at a concentration of 10.1 mg/ml of a palladium-*meso*-tetra(4-carboxyphenyl)porphyrin (Porphyrin Products, Logan, UT). P_{O_2} measurements were made 20 min after porphyrin injection, allowing it to be distributed to all the tissues.

In our system, intravascular measurements are made by placing an optical rectangular window (5 × 40 μm) within the vessel of interest, with the longest side of the rectangular slit positioned parallel to the vessel wall. Tissue P_{O_2} is measured in regions void of large vessels within intercapillary spaces with an optical window size of ~10 × 10 μm, which allows us to precisely establish the localization of the P_{O_2} measurements in arterioles, venules, and the interstitium (20). The phosphorescence decay due to quenching at a specific P_{O_2} yields a single decay constant, and in vitro calibration has been demonstrated to be valid for in vivo measurements. Intravascular and perivascular P_{O_2} measurements were made in the arterioles studied, and intravascular P_{O_2} measurements were made in venules. Interstitial tissue P_{O_2} was measured in regions distant from visible underlying and adjacent vessels.

Tissue oxygen delivery and extraction. The microvascular methodology used in our studies allows a detailed analysis of oxygen supply in the tissue. Calculations of O_2 delivery, defined as the amount of oxygen delivered by the arterioles to the microcirculation per unit time normalized relative to baseline, and O_2 extraction, defined as the amount of oxygen released by blood to the tissue by the microcirculation per unit time normalized relative to baseline, were made using *Eqs. 1* and *2*:

$$O_2\ \text{delivery} = \{(RBC_{Hb} \times \gamma \times Sa_{RBC}\%) + (HbV_{Hb} \times \gamma \times Sa_{HbV}\%) + (1 - Hct) \times \alpha \times Pa_{O_2}\} \times Q \quad (1)$$

$$O_2\ \text{extraction} = \{[RBC_{Hb} \times \gamma \times S(a - v)_{RBC}\%] + [HbV_{Hb} \times \gamma \times S(a - v)_{HbV}\%] + (1 - Hct) \times \alpha \times P(a - v)_{O_2}\} \times Q \quad (2)$$

where RBC_{Hb} is the [Hb] in RBC (expressed in g/dl of blood), HbV_{Hb} is the [Hb] in HbV (expressed in g/dl of blood), γ is the oxygen-carrying capacity of Hb at 100% saturation (or 1.34 ml O_2/g Hb), Sa% indicates the arteriolar oxygen saturation of RBC or HbV, S(a-v)% indicates the arteriovenous difference in oxygen saturation of RBC or HbV, (1 − Hct) is the fractional plasma volume (and converts the equation from units per dl of plasma to per dl of blood), α is the solubility of oxygen in plasma and is equal to 3.14 × 10^{-3} ml O_2/dl plasma mmHg, Pa_{O_2} is the arteriolar partial pressure of oxygen, $P(a\text{-}v)_{O_2}$ is the arteriovenous difference in P_{O_2}, and Q is the microvascular flow for each microvessel as a percentage of baseline. The oxygen dissociation curves were determined as described before. In this analysis, microvascular Hct was corrected according to the findings of Lipowsky and Firrell (10).

Experimental procedure. Baseline systemic, microvascular, and hemodynamic characterizations were performed before the start of the exchange. After each exchange and a stabilization period of 10 min, systemic and/or microvascular measurements were performed. Exchanges began every hour. After the *level 3* exchange transfusion, the same measurements were repeated, and then the P_{O_2} distribution was determined using phosphorescence-quenching microscopy (9). The duration of the experiment was 3–4 h.

Data analysis. Results are presented as means ± SD unless otherwise noted. All data are presented as absolute values and ratios relative to baseline values. A ratio of 1.0 signifies no change from baseline, whereas lower and higher ratios are indicative of changes proportionally higher or lower than baseline. The same vessels and functional capillary fields were followed so that direct comparisons to their baseline levels could be performed, allowing for more robust statistics for small sample populations. For repeated measurements, time-related changes were assessed by analysis of variance (ANOVA). Data within each group were analyzed using ANOVA for nonparametric repeated measurement, and when appropriate, post hoc analyses were performed with the Dunn's multiple comparison tests. For *level 3* exchange, groups were analyzed using one-way ANOVA, and post hoc analyses were performed with the Bonferroni post tests. All statistics were calculated using GraphPad Prism 4.01 (GraphPad Software, San Diego, CA). Changes were considered statistically significant if $P < 0.05$.

RESULTS

Exchange transfusion. Twenty-four animals (55–65 g body wt) entered into the exchange-transfusion (hemodilution) protocol, and all tolerated the experiment without any visible discomfort. Microvascular studies were completed in six preparations for each test material, namely, the *level 2* rHSA, HbV_8, and HbV_{29}. The data were analyzed using a model for computing oxygen delivery to the tissue at the microscopic level.

Hematological changes. The exchange-transfusion protocol resulted in a final Hct ranging from 11.0 ± 0.5 to 11.4 ± 0.6%. The HbV_8 and HbV_{29} groups had a final plasma Hb concentration of 2.1 ± 0.1 g/dl, which increased the total Hb concentration in blood (RBC + Hb in plasma) to 5.7 ± 0.2–0.3 g/dl after completion of the *level 3* exchange transfusion. Thus oxygen-carrying capacities at this level were similar to those found at *level 2*, where total blood Hb concentration was 5.7 ± 0.3 g/dl (Hct 18.1 ± 0.7) (Table 2).

Systemic and blood gas parameters. Changes in the systemic parameters are presented in Fig. 3. Mean arterial pressure was statistically lower for the extreme hemodilution tests with rHSA and the HbV_{29} group and attained the highest value with HbV_8 viscosity. Heart rate after hemodilution followed by exchange transfusion with the HbV solutions was ~10% higher than baseline at the *level 3* exchange. The slight increase in heart rate was not statistically different.

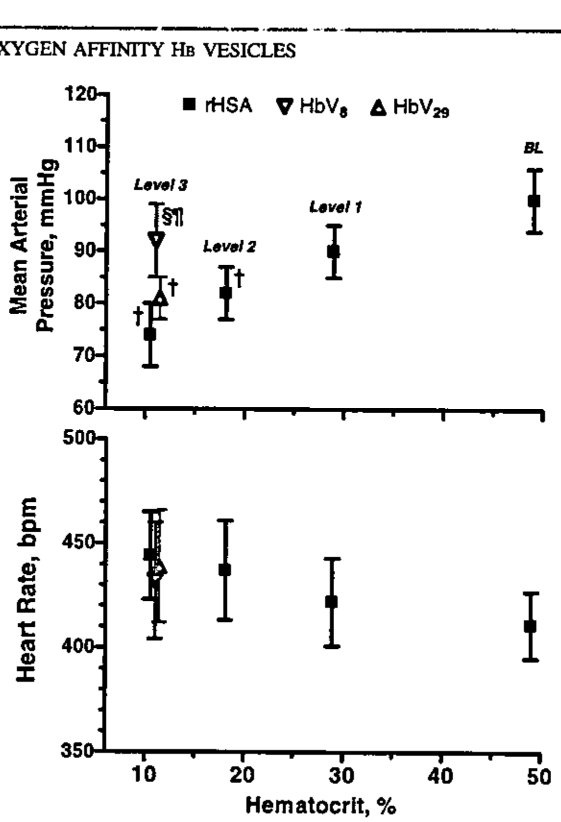

Fig. 3. Mean arterial blood pressure and heart rate [in beats/min (bpm)] at baseline (BL) (Hct 49%) and *level 1* (Hct 29%), *level 2* (Hct 18%), and *level 3* (Hct, 11%) hemodilutions. *Level 1* and *level 2* exchanges were performed with 5% rHSA as diluent. *Level 3* exchange was used to evaluate the oxygen transport of HbV_8 vs. HbV_{29} and rHSA. †$P < 0.05$ relative to baseline; §$P < 0.05$ relative to *level 3* rHSA; ¶$P < 0.05$, *level 3* with HbV_8 vs. *level 3* with HbV_{29}.

Analysis of arterial blood gases (Table 2) showed a statistical increase in P_{O_2} after hemodilution and exchange transfusion. Pa_{CO_2} was unchanged from baseline after hemodilution. Blood pH was not statistically changed. At *level 3* exchange, BE was positive and not statistically different between HbV groups, but it was negative and statistically different from baseline for the rHSA group ($P < 0.05$).

Colligative properties. Blood viscosities and COP after *level 3* exchange were sampled at 1 h and 10 min after completion

Table 2. *Laboratory parameters during exchange protocol*

		Level 1 Hemodilution	*Level 2* Hemodilution	*Level 3* Hemodilution		
	Baseline	rHSA	rHSA	rHSA	HbV_8	HbV_{29}
n	24	24	24	6	6	6
Hct, %	48.8±1.2	28.8±0.8*	18.1±0.7*	11.1±0.8*	11.0±0.5*	11.4±0.6*
Hb, g/dl						
Whole blood	14.8±0.4	9.0±0.5*	5.7±0.3*	3.7±0.4*	5.7±0.2*†	5.7±0.3*†
Plasma					2.1±0.1	2.1±0.1
Pa_{O_2}, mmHg	59.2±4.6	68.7±5.2	73.5±3.7*	87.5±7.0*	77.1±4.3*†	76.4±4.4*†
Pa_{CO_2}, mmHg	49.2±3.6	52.4±6.7	49.0±3.5	42.0±3.2*	53.0±3.9†‡	46.8±4.3
Arterial pH	7.35±0.02	7.35±0.03	7.37±0.03	7.38±0.04	7.35±0.03	7.36±0.03
HCO_3, mM	27.9±2.3	28.5±3.5	27.6±2.2	24.8±2.5	28.2±2.6	25.8±2.1
BE, mM	3.2±2.0	3.4±2.4	2.9±2.1	−0.2±1.9*	3.1±1.7†	1.0±2.0

Values are means ± SD. Baseline values include all animals in the study. No significant differences were detected between the baseline values of each group or between the values after *level 1* and *level 2* exchange before the exchange with test solutions. Hct, systemic hematocrit; Hb, hemoglobin content of blood; Pa_{O_2}, arterial partial O_2 pressure; Pa_{CO_2}, arterial partial pressure of CO_2; BE, base excess. *$P < 0.05$ compared with baseline; †$P < 0.05$ compared with *level 3* rHSA; ‡$P < 0.05$ compared with *level 3* HbV_8 to *level 3* HbV_{29}.

Table 3. *Rheological properties and COP*

Fluid	Blood Viscosity, cp	Plasma Viscosity, cp	COP, mmHg	*n*
Blood	4.2±0.7	1.2±0.1	17.6±0.7	6
Level 2 rHSA	2.0±0.2*	0.9±0.1	17.2±0.8	4
Level 3 rHSA	1.6±0.2*	0.9±0.1	17.4±1.1	5
Level 3 HbV_8	1.9±0.3*	1.0±0.1	17.3±0.8	6
Level 3 HbV_{29}	2.0±0.4*	1.0±0.1	17.8±1.0	5

Values are means ± SD; *n* = no. of animals studied. Viscosity was measured at a shear rate of 160 s^{-1} at 37°C. COP was measured at 27°C. Hct are presented in Table 2. *$P < 0.05$ compared with nondiluted blood.

of the exchange. Table 3 shows that blood viscosity ranges from 1.6 cp (plasma 0.9 cp) for rHSA to 2.0 cP (plasma 1.0 cp) for the HbV groups.

All test materials caused COP to maintain the value for normal blood for this species (5), namely, 17.6 ± 0.7 mmHg at 1 h after the last exchange, showing that introduction of bulk solutions into the circulation caused minor fluid shifts.

Microhemodynamics. After *level 3* exchange, arteriolar and venular diameters were not statistically different from baseline for any of the groups. Arteriolar flow velocities attained the highest value for the HbV_8 group, being 1.90 relative to baseline, which was statistically significant. The same effect was found in the venular microcirculation, where blood flow velocity was 2.20 relative to baseline. HbV_{29} exchange transfusion lowered both arteriolar and venular velocities relative to the values attained at the *level 2* exchange. However, venular velocity in this group was statistically significantly higher than in baseline. Notably, the *level 2* hemodilution with rHSA caused significantly higher blood flow velocities in the arteriolar and venular microcirculation (Fig. 4).

Combining data for the RBC flow velocity and diameter allowed calculation of the arteriolar and venular blood flows (Fig. 5). The results of this calculation showed that all exchanges caused blood flow to increase. Arteriolar and venular blood flows at *level 2* exchange with the use of rHSA were significantly higher than those at baseline. However, continuing hemodilution with this material to *level 3* exchange did not sustain the increase, and arteriolar and venular blood flow, although showing a tendency to remain elevated, were not statistically different from baseline values.

Level 3 exchange transfusion with HbV_8 and HbV_{29} caused blood flow to be significantly higher than baseline. Furthermore, the HbV_8 group showed consistently higher blood flows than the HbV_{29} group; however, the trend was not statistically significant.

Functional capillary density. The number of capillaries with RBC passage upon *level 3* hemodilution in the rHSA, HbV_8, and HbV_{29} groups was 62 ± 9, 76 ± 12, and 72 ± 13% of baseline, respectively. These values were statistically different from baseline but not statistically different with respect to each other (Fig. 6).

Microvascular oxygen distribution. Oxygen tension measured using phosphorescence microscopy after *level 3* exchange transfusion in the rHSA, HbV_8, and HbV_{29} groups showed that these materials produced virtually identical distributions of arteriolar microvascular P_{O_2} (arterioles averaged 49.5 mmHg), although HbV_8 tended to be higher (Fig. 7). The decrease of RBC from *level 2* to *level 3* did not decrease the arteriolar P_{O_2}. Venular P_{O_2} after *level 3* was significantly lower than at *level 2* exchange in all cases (rHSA, 7.2 ± 3.2 mmHg; HbV_8, 15.1 ± 3.7 mmHg; HbV_{29}, 9.6 ± 4.2 mmHg).

Tissue P_{O_2} values at *level 3* exchange were consistently lower than those at *level 2* exchange (20.1 ± 2.2 mmHg), with the difference being statistically significant. The highest was attained by the HbV_8 group, being 14.0 ± 2.2 mmHg. By comparison, tissue P_{O_2} for the HbV_{29} group was 9.2 ± 2.7 mmHg and for the rHSA group, 2.6 ± 1.4 mmHg, which was significantly lower compared with the HbV_8 and HbV_{29} groups (Fig. 7).

Oxygen delivery and extraction. Figure 8 shows the results of the analysis for delivery and release of oxygen by the

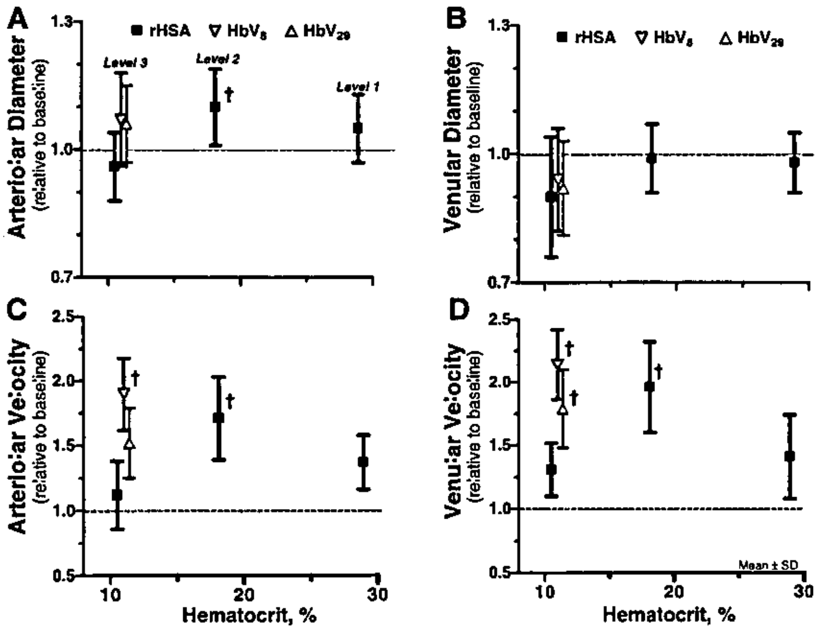

Fig. 4. Changes relative to baseline in arteriolar and venular hemodynamics at the *level 1*, *level 2*, and *level 3* exchanges. Dashed lines represent baseline level. †$P < 0.05$ relative to baseline. Arteriolar (*A*) and venular (*B*) diameters (μm, means ± SD, *n* = no. of vessels studied) in each animal group were as follows. Baseline: arterioles (A), 61.2 ± 10.2, *n* = 80; venules (V), 62.0 ± 12.3, *n* = 80. *Level 1* with rHSA: A, 65.6 ± 12.4; V, 61.1 ± 12.4. *Level 2* with rHSA: A, 66.1 ± 14.6; V, 64.3 ± 15.2. *Level 3* with rHSA: A, 63.7 ± 14.4, *n* = 20; V, 61.0 ± 16.7, *n* = 20. *Level 3* with HbV_8: A, 64.9 ± 15.7, *n* = 20; V, 64.6 ± 18.2, *n* = 20. *Level 3* with HbV_{29}: A, 66.1 ± 16.2, *n* = 20; V, 63.1 ± 18.0, *n* = 20. Arteriolar (*C*) and venular (*D*) RBC velocities (mm/s, means ± SD) in each animal group were as follows. Baseline: A, 4.9 ± 1.3; V, 1.7 ± 0.5. *Level 1* with rHSA: A, 6.3 ± 1.4; V, 2.0 ± 0.7. *Level 2* with rHSA: A, 7.9 ± 1.5; V, 2.6 ± 0.9. *Level 3* rHSA: A, 5.2 ± 2.0, *n* = 20; V, 1.9 ± 1.1, *n* = 20. *Level 3* with HbV_8: A, 7.2 ± 1.8, *n* = 20; V, 3.3 ± 1.0, *n* = 20. *Level 3* with HbV_{29}: A, 7.0 ± 1.7, *n* = 20; V, 3.0 ± 0.9, *n* = 20.

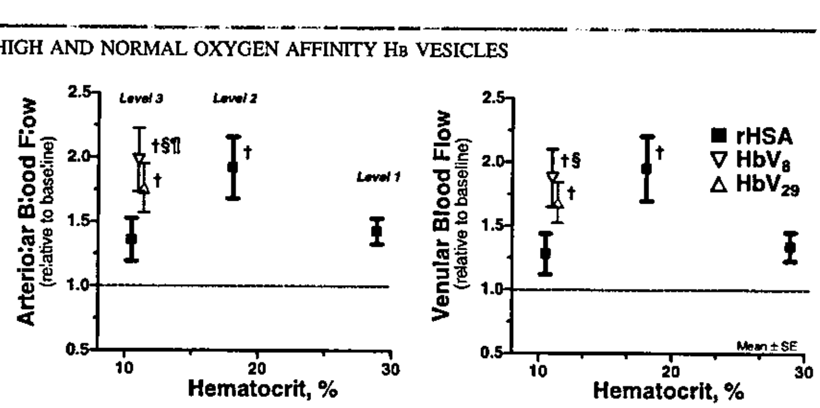

Fig. 5. Arteriolar and venular flow (nl/s, means ± SD, n = no. of vessels studied) in each animal group were as follows. Baseline: arterioles (A), 14.8 ± 7.1, n = 76; venules (V), 5.0 ± 2.9, n = 76. *Level 1* with rHSA: A, 21.9 ± 9.7; V, 5.8 ± 3.6. *Level 2* with rHSA: A, 27.2 ± 16.1; V, 8.3 ± 4.2. *Level 3* with rHSA: A, 16.9 ± 6.8, n = 20; V, 5.4 ± 4.8, n = 20. *Level 3* with HbV_8: A, 23.4 ± 8.1, n = 18; V, 9.9 ± 5.1, n = 18. *Level 3* with HbV_{29}: A, 21.0 ± 8.0, n = 18; V, 8.3 ± 5.2, n = 18.

microcirculation. It is apparent that exchanging RBC for HbV_8 maintains oxygen delivery to the tissue, whereas HbV_{29} reduces this by ~20%, and continued hemodilution with a non-oxygen-carrying material significantly depresses oxygen delivery to the tissue, reducing this to half of that attained at the *level 2* hemodilution.

DISCUSSION

The principal finding of this study is that under identical extreme hemodilution conditions, with the use of vesicles encapsulating Hb with normal P_{50} (HbV_{29} = 29 mmHg) and low P_{50} (HbV_8 = 8 mmHg), tissue Po_2 is statistically significantly higher when the high oxygen affinity material is used, namely, 14.0 ± 2.2 vs. 9.2 ± 2.7 mmHg. The significantly increased tissue Po_2 attained with HbV_8 appears to be due to a series of incremental improvements in microvascular and macrovascular hemodynamics comprising the increase of arteriolar blood flow and mean arterial blood pressure, which was significantly higher ($P < 0.05$) for HbV_8 than for HbV_{29}.

In the hemodilution procedures of this study, blood was exchanged with a rHSA solution as a colloidal plasma expander, which was the same suspending medium used for the Hb vesicles. Therefore, in these experiments, we can make a direct comparison between an oxygen-carrying and non-oxygen-carrying blood substitute, uncomplicated by the presence of additional materials. Our results show that the *level 2* hemodilution with rHSA leads to maintained functional capillary density and significantly improved arteriolar and venular blood flow, although somewhat lowered central blood pressure. The latter finding is not necessarily negative and may reflect a lowered overall peripheral vascular resistance due to the decrease of blood viscosity after hemodilution. The fact that microvascular flow is significantly increased indicates that the *level 2* hemodilution with rHSA provides the tissue with adequate microvascular perfusion and that this colloid is an adequate plasma expander.

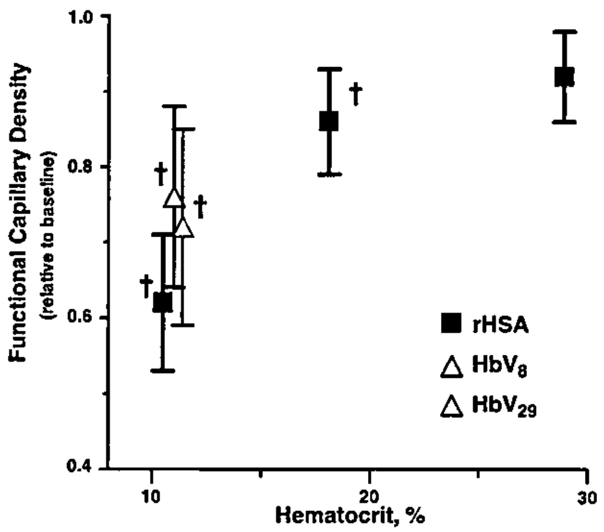

Fig. 6. Functional capillary density after the *level 1*, *level 2*, and *level 3* exchanges for the different test fluids. All values are relative to baseline levels. †$P < 0.05$ relative to baseline.

Average oxygen delivery and extraction were somewhat greater for HbV_8 than for HbV_{29}. These are calculated values and are not statistically significantly different; however, the same difference was found in all micro and macro parameters measured in this study.

The *level 2* hemodilution and the succeeding *level 3* hemodilution with either HbV_8 and HbV_{29} resulted in the same total Hb concentration in the circulation (5.7 and 5.8 g Hb/dl); however, oxygen delivery was lower with HbV_{29} and lowest with rHSA, as might be expected due to the low Hb content (3.7 g Hb/dl) in the absence of plasma Hb for the rHSA group. Therefore, because all groups had the same Hct at the *level 3* hemodilution, the sustained oxygen consumption and tissue Po_2 relative to the rHSA group clearly demonstrate that Hb vesicles release oxygen. However, the vesicles with the lowest P_{50} provide an oxygen delivery capacity identical to that of blood at *level 2* hemodilution, whereas vesicles with a high P_{50} lower oxygen delivery at the microcirculatory level, an effect probably caused by the decreased blood flow associated with HbV_{29}.

The differences in tissue Po_2, mean arterial blood pressure, and arteriolar blood flow between HbV_8 and HbV_{29} show that in designing a blood substitute, it is not sufficient to provide adequate oxygen-carrying capacity. Once a suitable oxygen carrier is available, it also must be able to maintain or enhance other circulatory transport parameters, particularly flow. The Hb vesicles used in this study are vasoinactive, and the difference in P_{50} appears to be a factor in improving flow condition that is not related to vasoactivity. An explanation for this may be related to the inherent variability of tissue Po_2 shown in this and other studies (4, 22), which may be enhanced in extreme hemodilution. This variability determines that if average tissue Po_2 is low, portions of the tissue may become anoxic. Introducing a small quantity of a low-P_{50} Hb oxygen carrier into the circulation will deliver oxygen only to those parts of the tissue

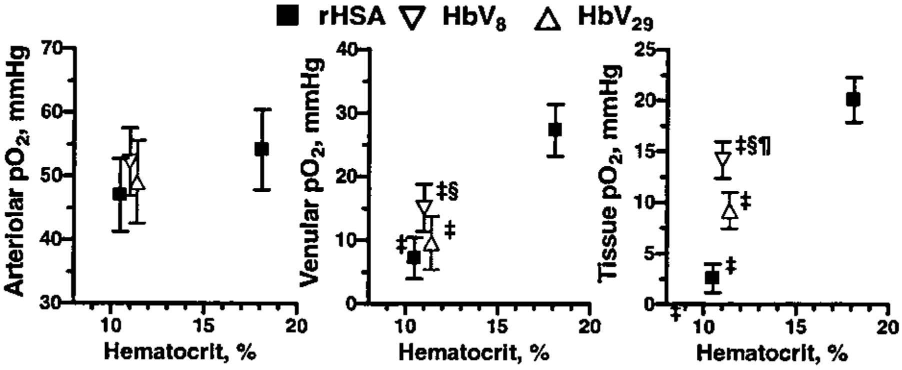

Fig. 7. Intravascular Po_2 after the *level 2* and *level 3* hemodilutions. Values are presented as means ± SD. ‡$P < 0.05$ compared with *level 2* with rHSA; §$P < 0.05$ compared with *level 3* with rHSA; ¶$P < 0.05$, *level 3* with HbV_8 vs. *level 3* with HbV_{29}.

where the anoxic threshold is passed, thus eliminating the inherent variability of oxygen delivery shown by the variability of tissue Po_2.

Considering the significantly improved blood pressure and the trend toward higher flow for HbV_8 (in the absence of vasoconstriction and changes in the rheological properties of blood), it is possible that in conditions of extreme hemodilution the cardiac function should be improved because of the proposed more homogenous heart tissue oxygenation using HbV_8 vs. HbV_{29}.

In summary, the present results show that either HbV_8 or HbV_{29} are efficient oxygen carriers that do not cause vasoactivity. The experiments were carried out using rHSA as a hemodiluent, and this material was adequate as a plasma volume substitute. Oxygen extraction was similar for both oxygen carriers; however, HbV_8 appeared to be beneficial at the systemic level, because base excess remained at baseline levels, whereas it was decreased for HbV_{29}. This finding suggests that improved tissue Po_2 and microcirculatory oxygen delivery may be efficient in other tissues. The improvement obtained may be specific to the conditions of these experiments in which the vesicles were tested for their capacity to restore tissue Po_2, FCD, and oxygen extraction in the microcirculation during extreme hemodilution. The significant differences in the tissue oxygen parameters produced by the presence of low-P_{50} Hbs vs. an identical oxygen carrier with normal P_{50} suggests that small amounts of Hbs with high oxygen affinity may have therapeutic effects in the treatment of ischemic conditions (6).

ACKNOWLEDGMENTS

We greatly acknowledge A. Barra and C. Walter (Univ. of California-San Diego) for technical assistance and Drs. K. Sou and Y. Teramura (Waseda University) for preparation of the HbV suspension.

GRANTS

This work was supported by National Heart, Lung, and Blood Institute (NHLBI) Bioengineering Research Partnership Grant R24-HL-64395, NHLBI Grants R01-HL-62354 and R01-HL-62318 (to M. Intaglietta), and NHLBI Program Project Grant P01-HL-71064-01 (to Dr. J. Friedman) and by U.S. Army Grant PR023085, Health Sciences Research Grants (Research on Regulatory Science), the Ministry of Health, Labour, and Welfare, Japan, and grants in aid for Scientific Research from the Japan Society for the Promotion of Science (B16300162).

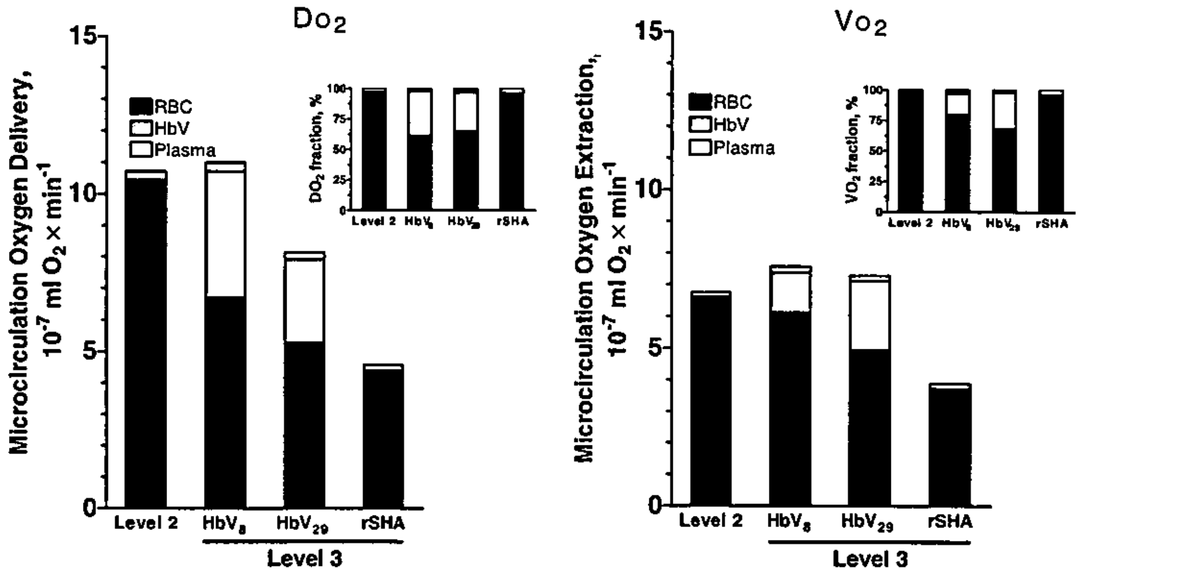

Fig. 8. Arterial oxygen delivery (Do_2) and extraction (Vo_2) before and after the *level 3* hemodilution. Calculations of global oxygen transport are not directly measurable in our model; however, the changes relative to baseline can be calculated using the measured parameters. These calculations can be identified as those presented without standard deviations to focus on their tendencies rather than on the variability of the measurement.

REFERENCES

1. **Altman DG and Bland JM.** Statistics notes: how to randomise. *BMJ* 319: 703–704, 1999.
2. **Baines AD and Drangova R.** Does dopamine use several signal pathways to inhibit Na-Pi transport in OK cells? *J Am Soc Nephrol* 9: 1604–1612, 1998.
3. **Baines AD and Ho P.** O_2 affinity of cross-linked hemoglobins modifies O_2 metabolism in proximal tubules. *J Appl Physiol* 95: 563–570, 2003.
4. **Cabrales P, Kanika ND, Manjula BN, Tsai AG, Acharya SA, and Intaglietta M.** Microvascular P_{O_2} during extreme hemodilution with hemoglobin site specifically PEGylated at Cys-93(β) in hamster window chamber. *Am J Physiol Heart Circ Physiol* 287: H1609–H1617, 2004.
5. **Cabrales P, Tsai AG, and Intaglietta M.** Microvascular pressure and functional capillary density in extreme hemodilution with low and high plasma viscosity expanders. *Am J Physiol Heart Circ Physiol* 287: H363–H373, 2004.
6. **Endrich B, Asaishi K, Götz A, and Messmer K.** Technical report: a new chamber technique for microvascular studies in unanaesthetized hamsters. *Res Exp Med (Berl)* 177: 125–134, 1980.
7. **Hogan MC, Bebout DE, and Wagner PD.** Effect of increased Hb-O_2 affinity on $V_{O_2\,max}$ at constant O_2 delivery in dog muscle in situ. *J Appl Physiol* 70: 2656–2662, 1991.
8. **Intaglietta M, Silverman NR, and Tompkins WR.** Capillary flow velocity measurements in vivo and in situ by television methods. *Microvasc Res* 10: 165–179, 1975.
9. **Kerger H, Groth G, Kalenka A, Vajkoczy P, Tsai AG, and Intaglietta M.** pO_2 measurements by phosphorescence quenching: characteristics and applications of an automated system. *Microvasc Res* 65: 32–38, 2003.
10. **Lipowsky HH and Firrell JC.** Microvascular hemodynamics during systemic hemodilution and hemoconcentration. *Am J Physiol Heart Circ Physiol* 250: H908–H922, 1986.
11. **Lipowsky HH and Zweifach BW.** Application of the "two-slit" photometric technique to the measurement of microvascular volumetric flow rates. *Microvasc Res* 15: 93–101, 1978.
12. **Sakai H, Hara H, Yuasa M, Tsai AG, Takeoka S, Tsuchida E, and Intaglietta M.** Molecular dimensions of Hb-based O_2 carriers determine constriction of resistance arteries and hypertension. *Am J Physiol Heart Circ Physiol* 279: H908–H915, 2000.
13. **Sakai H, Masada Y, Horinouchi H, Yamamoto M, Ikeda E, Takeoka S, Kobayashi K, and Tsuchida E.** Hemoglobin-vesicles suspended in recombinant human serum albumin for resuscitation from hemorrhagic shock in anesthetized rats. *Crit Care Med* 32: 539–545, 2004.
14. **Sakai H, Tomiyama KI, Sou K, Takeoka S, and Tsuchida E.** Polyethyleneglycol-conjugation and deoxygenation enable long-term preservation of hemoglobin-vesicles as oxygen carriers in a liquid state. *Bioconjug Chem* 11: 425–432, 2000.
15. **Sakai H, Tsai AG, Intaglietta M, and Tsuchida E.** Hemoglobin encapsulation with polyethylene glycol-modified and unmodified vesicles: systemic and microvascular hemodynamics at 80% blood substitution. In: *Advances in Blood Substitutes. Industrial Opportunities and Medical Challenges*, edited by Winslow RM, Vandegriff KD, and Intaglietta M. Boston, MA: Birkhäuser, 1997, p. 151–166.
16. **Sakai H, Tsai AG, Rohlfs RJ, Hara H, Takeoka S, Tsuchida E, and Intaglietta M.** Microvascular responses to hemodilution with Hb vesicles as RBC substitutes: influence of O_2 affinity. *Am J Physiol Heart Circ Physiol* 276: H553–H562, 1999.
17. **Sou K, Endo T, Takeoka S, and Tsuchida E.** Poly(ethylene glycol)-modification of the phospholipid vesicles by using the spontaneous incorporation of poly(ethylene glycol)-lipid into the vesicles. *Bioconjug Chem* 11: 372–379, 2000.
18. **Torres Filho IP and Intaglietta M.** Microvessel P_{O_2} measurements by phosphorescence decay method. *Am J Physiol Heart Circ Physiol* 265: H1434–H1438, 1993.
19. **Tsai AG.** Influence of cell-free hemoglobin on local tissue perfusion and oxygenation after acute anemia after isovolemic hemodilution. *Transfusion* 41: 1290–1298, 2001.
20. **Tsai AG, Friesenecker B, Mazzoni MC, Kerger H, Buerk DG, Johnson PC, and Intaglietta M.** Microvascular and tissue oxygen gradients in the rat mesentery. *Proc Natl Acad Sci USA* 95: 6590–6595, 1998.
21. **Tsai AG, Friesenecker B, McCarthy M, Sakai H, and Intaglietta M.** Plasma viscosity regulates capillary perfusion during extreme hemodilution in hamster skin fold model. *Am J Physiol Heart Circ Physiol* 275: H2170–H2180, 1998.
22. **Tsai AG, Vandegriff KD, Intaglietta M, and Winslow RM.** Targeted O_2 delivery by low-P_{50} hemoglobin: a new basis for O_2 therapeutics. *Am J Physiol Heart Circ Physiol* 285: H1411–H1419, 2003.
23. **Webb AR, Barclay SA, and Bennett ED.** In vitro colloid osmotic pressure of commonly used plasma expanders and substitutes: a study of the diffusibility of colloid molecules. *Intensive Care Med* 15: 116–120, 1989.

Lippincott Williams & Wilkins

Critical Care Medicine

OFFICIAL JOURNAL OF THE SOCIETY OF CRITICAL CARE MEDICINE

Title: New generation of hemoglobin-based oxygen carriers evaluated for oxygenation of critically ischemic hamster flap tissue

Author(s): Claudio Contaldo MD; Jan Plock MD; Hiromi Sakai PhD; Shinji Takeoka PhD; Eishun Tsuchida PhD; Michael Leunig MD; Andrej Banic MD, PhD; Dominique Erni MD

Objectives: The aim of this study was to investigate and compare the effects of a traditionally formulated, low-viscosity, right-shifted polymerized bovine hemoglobin solution and a highly viscous, left-shifted hemoglobin vesicle solution (HbV-HES) on the oxygenation of critically ischemic peripheral tissue.

Design: Randomized, prospective study.

Setting: University laboratory.

Subject: A total of 40 male golden Syrian hamsters.

Interventions: Island flaps were dissected from the back skin of anesthetized hamsters. The flap included a critically ischemic, hypoxic area that was perfused via a collateralized vasculature. One hour after completion of the preparation, the animals received a 33% blood exchange with 6% hydroxyethyl starch 200/0.5 (HES, n = 9), HbV suspended in HES (HbV-HES, n = 8), or polymerized bovine hemoglobin solution (n = 9).

Measurements and Main Results: Three hours after the blood exchange, microcirculatory blood flow (laser-Doppler flowmetry) was increased to 262% of baseline for HbV-HES (p < .01) and 197% for polymerized bovine hemoglobin solution (p < .05 vs. baseline and HbV-HES). Partial tissue oxygen tension (bare fiber probes) was only improved after HbV-HES (9.4 torr to 14.2 torr, p < .01 vs. baseline and other groups). The tissue lactate/pyruvate ratio (microdialysis) was elevated to 51 in the untreated control animals, and to 34 ± 8 after HbV-HES (p < .05 vs. control) and 38 ± 11 after polymerized bovine hemoglobin solution (not significant).

Conclusions: Our study suggests that in critically ischemic and hypoxic collateralized peripheral tissue, oxygenation may be improved by normovolemic hemodilution with HbV-HES. We attributed this improvement to a better restoration of the microcirculation and oxygen delivery due to the formulation of the solution.

ARTICLE

OBC
www.rsc.org/obc

Synthesis of protoheme IX derivatives with a covalently linked proximal base and their human serum albumin hybrids as artificial hemoprotein

Akito Nakagawa, Naomi Ohmichi, Teruyuki Komatsu and Eishun Tsuchida*
Advanced Research Institute for Science and Engineering, Waseda University, 3-4-1 Ohkubo, Shinjuku-ku, Tokyo 169-8555, Japan. E-mail: eishun@waseda.jp; Fax: +81 3-3205-4740; Tel: +81 3-5286-3120

Received 15th June 2004, Accepted 3rd September 2004
First published as an Advance Article on the web 27th September 2004

The simple one-pot reaction of protoporphyrin IX and ω-(*N*-imidazolyl)alkylamine or *O*-methyl-L-histidyl-glycine with benzotriazol-1-yl-oxytris(dimethylamino)phosphonium hexafluorophosphate at room temperature produced a series of protoporphyrin IX species with a covalently linked proximal base at the propionate side-chain. The central iron was inserted by the general $FeCl_2$ method, converting the free-base porphyrins to the corresponding protoheme IX derivatives. Mesoporphyrin IX and diacetyldeuteroporphyrin IX analogues were also prepared by the same procedure. The Fe(II) complexes formed dioxygen (O_2) adducts in dimethylformamide at 25 °C. Some of them were incorporated into the hydrophobic domain of recombinant human serum albumin (rHSA), providing albumin–heme hybrids (rHSA–heme), which can bind and release O_2 in aqueous media (pH 7.3, 25 °C). The oxidation process of converting the dioxygenated heme in rHSA to the inactive Fe(III) state obeyed first-order kinetics, indicating that the μ-oxo dimer formation was prevented by the immobilization of heme in the albumin scaffold. The rHSA–heme, in which the histidylglycil tail coordinates to the Fe(II) center, showed the most stable O_2 adduct complexes.

Introduction

Numerous model compounds of hemoglobin (Hb) and myoglobin (Mb) have already been prepared and their O_2-binding equilibria and kinetics were extensively studied.[1] In particular, synthetic hemes having a sterically encumbered porphyrin platform can form stable O_2 adducts in organic solvent at room temperature. If we are to reproduce or mimic any biochemical reaction, the aqueous medium is particularly important. The dioxygenated complexes of highly-modified hemes are unfortunately oxidized to the ferric state in water. Human serum albumin (HSA) is the most abundant plasma protein in our circulatory system and solubilizes hydrophobic small molecules.[2] We have found that synthetic hemes are also spontaneously incorporated into HSA, which provides unique albumin–heme hybrids (HSA–hemes) and allows their Fe(II) states to remain stable in aqueous solution.[3] Actually, recombinant HSA[4] (rHSA) including tetrakis(α,α,α,α-*o*-pivalamidophenyl)porphinatoiron(II) with a covalently linked proximal base can reversibly bind and release O_2 under physiological conditions, and acts as an artificial O_2 transporter in the blood stream.[5] Our next target is to realize O_2 coordination to rHSA–heme involving protoheme IX in the same manner as natural Hb and Mb. The dioxygenation of protoheme IX has several advantages. (1) Synthetic procedures are rather simplified with respect to the highly modified tetraphenylporphyrin. (2) It has the same structure and thus the same spectra as do hemoproteins; this makes possible the study of subtle changes in the protein nanostructure. (3) Its metabolism process has been clarified,[6] which is an advantage for medical use as an artificial O_2 carrier.

We report herein the simple synthetic methodology of protoheme IX derivatives with a covalently-linked proximal imidazolyl arm and the O_2-binding properties of the obtained rHSA–hemes.

Results and discussion

Synthesis

The free-base porphyrins with a covalently linked proximal base (**1a**–**8a**, Scheme 1) were synthesized by the one-pot reaction of protoporphyrin IX, ω-(*N*-imidazolyl)alkylamine [R_2H; 3-(*N*-imidazolyl)propylamine, 4-(*N*-(2-methylimidazolyl))-butylamine or *O*-methyl-L-histidyl-glycine] for one propionic acid group, and a capping alcohol or amine on the other side (R_3H; MeOH, EtOH or $MeNH_2$) in the presence of benzotriazol-1-yl-oxytris(dimethylamino)phosphonium hexafluorophosphate (BOP) at 25 °C in pyridine [or dimethylformamide (DMF)] (Scheme 2). The carbonyl attachment was made through either an ester or an amide function. After the reaction, the mixture was poured into 10% NaCl solution, which led to the precipitation of the crude porphyrin. Centrifugation at 7000 g for 30 min gave a purple pellet. The pyridine (or DMF), BOP, R_2H and R_3H in the supernatant were all discarded at this point. The obtained precipitate was dissolved in $CHCl_3$ and showed several spots on a thin layer chromatograph. The anpolar band corresponds to the double R_3-substituted component (ex. protoporphyrin IX diethyl ester in the cases of **2**, **5**, **6**) and the second band is the desired porphyrin, which is purified by a silica gel chromatographic separation (yield: 20–30%). The iron was then inserted by the general $FeCl_2$ method with 2,6-lutidine in DMF solution, giving the corresponding hemins. Mesoporphyrin IX and diacetyldeuteroporphyrin IX also gave similar analogues (**7b** and **8b**). We obtained a mixture of two isomeric compounds that we were unable to separate.

Traylor and co-workers reported many pioneering studies on "chelated hemes".[7] They synthesized compound **1b**, for instance, using an acid anhydride procedure directly from protohemin chloride.[7e] First, the protohemin dimethyl ester was partially hydrolyzed and, after purification, the mono acid was coupled to a 3-(*N*-imidazolyl)propylamine by the pivaloyl chloride method. Nevertheless, reaction mixtures involving the diacid and monoacid are normally insoluble in common organic solvents, therefore, the yield of this reaction largely depends on the separation techniques. In contrast, our simple procedure makes it possible to synthesize a series of new protoporphyrins with a wide variety of proximal bases and end-capping groups of the other propionic acid.

Dioxygenation of heme in DMF solution

The obtained hemin complexes **1b**–**8b** in DMF solution were reduced to the corresponding Fe(II) complexes using a solution

DOI: 10.1039/b409017a

